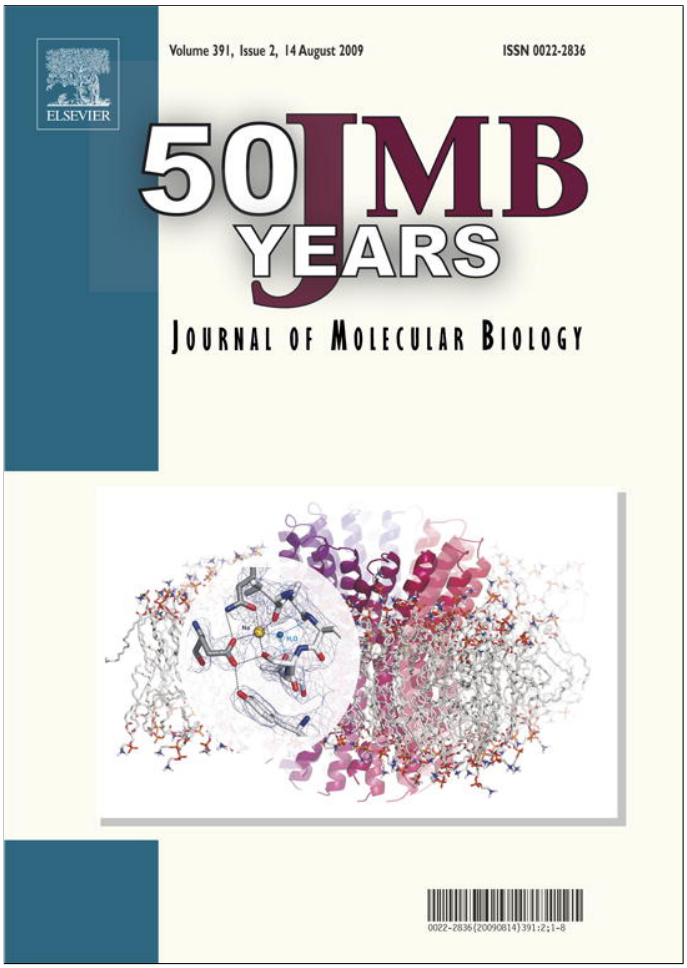

doi:10.1016/j.jmb.2009.06.041 J. Mol. Biol. (2009) 391, 282–300

JMB

Available online at www.sciencedirect.com

ScienceDirect

ELSEVIER

Nuclear Factor I Regulates Brain Fatty Acid-Binding Protein and Glial Fibrillary Acidic Protein Gene Expression in Malignant Glioma Cell Lines

Miranda Brun†, Jeffrey E. Coles†, Elizabeth A. Monckton, Darryl D. Glubrecht, Dwayne Bisgrove and Roseline Godbout*

Department of Oncology, Cross Cancer Institute, University of Alberta, 11560 University Avenue, Edmonton, Alberta, Canada T6G 1Z2

Received 30 January 2009; received in revised form 10 June 2009; accepted 15 June 2009
Available online 21 June 2009

Edited by M. Yaniv

Glial fibrillary acidic protein (GFAP), an intermediate filament protein normally found in astrocytes, and the radial glial marker brain fatty acid-binding protein (B-FABP; also known as FABP7) are co-expressed in malignant glioma cell lines and tumors. Nuclear factor I (NFI) recognition sites have been identified in the *B-FABP* and *GFAP* promoters, and transcription of both genes is believed to be regulated by NFI. Here, we study the role of the different members of the NFI family in regulating endogenous and ectopic *B-FABP* and *GFAP* gene transcription in human malignant glioma cells. We show by gel shifts that all four members of the NFI family (NFIA, NFIB, NFIC, and NFIX) bind to *B-FABP* and *GFAP* NFI consensus sites. Over-expression of NFIs, in conjunction with mutation analysis of NFI consensus sites using a reporter gene assay, supports a role for all four NFIs in the regulation of the *GFAP* and *B-FABP* genes. Knock-down of single or combined NFIs reveals promoter-dependent and promoter-context-dependent interaction patterns and suggests cross talk between the different members of the NFI family. Our data indicate that the NFI family of transcription factors plays a key role in the regulation of both the *B-FABP* and *GFAP* genes in malignant glioma cells.

Keywords: nuclear factor I; brain fatty acid-binding protein; glial fibrillary acidic protein; malignant glioma; gene regulation

Introduction

Malignant gliomas, comprising grade III and grade IV astrocytomas (also called anaplastic astrocytoma and glioblastoma multiforme, respectively), are the most common brain tumors in adults.[1] These highly invasive tumors are usually fatal within 2 years of diagnosis. Histopathological analysis of malignant gliomas has shown that increasing anaplasia correlates with reduced levels of the intermediate filament protein glial fibrillary acidic protein (GFAP).[2,3] Manipulation of GFAP levels in malignant glioma cells suggests an association between GFAP expression and a reduced transformed state.[4–9]

Brain fatty acid-binding protein (B-FABP; also known as FABP7 or BLBP) is a marker of radial glial cells.[10,11] B-FABP has been implicated in the establishment of the radial glial fiber system required for the migration of neurons to their correct location in the central nervous system and in glial cell differentiation.[10,11] It is generally believed that neural stem cells give rise to radial glial cells, which in turn become mature astrocytes once neuronal migration is complete.[12,13] However, radial glial cells can also give rise to neurons and have been proposed to function as neural stem cells.[14–16] B-FABP expression has recently been shown to be associated with increased cell migration in malignant glioma cells and with a worse clinical prognosis in high-grade astrocytomas.[17–19] Of note, malignant glioma cell lines that express B-FABP also express GFAP,

*Corresponding author. E-mail address: rgodbout@ualberta.ca.

† M.B. and J.E.C. contributed equally to this work.

Abbreviations used: GFAP, glial fibrillary acidic protein; B-FABP, brain fatty-acid-binding protein; NFI, nuclear factor I; AP-2, activating protein 2; CAT, chloramphenicol acetyltransferase; HA, hemagglutinin; br, binding region; ChIP, chromatin immunoprecipitation; RT-PCR, reverse transcription polymerase chain reaction; siRNA, small interfering RNA; PVDF, polyvinylidene fluoride.

suggesting either a functional or a regulatory link between these two proteins.[20]

Nuclear factor I (NFI) has been implicated in the regulation of both the *B-FABP* and the *GFAP* genes.[21–23] NFI is a family of transcription factors that includes four genes: *NFIA*, *NFIB*, *NFIC*, and *NFIX/NFID*.[24] Additional diversity within this family comes from alternative splicing and post-translational modification (reviewed in Ref. 25). NFI proteins bind to the consensus sequence 5′-TTGGCN$_5$GCCAA-3′ as homodimers or heterodimers with the same apparent affinity.[26,27] NFIs are widely expressed in different tissues and cell types, although the distribution pattern of each NFI varies from tissue to tissue.[28] NFI consensus binding sites are found in many brain-specific gene promoters/enhancers, and NFI transcription factors have been proposed to play a role in the determination of gene expression in glial cells.[29–34]

The *B-FABP* promoter has at least two NFI recognition elements located within 500 bp of the *B-FABP* transcription start site. Using a combination of gel-shift assays and potato acid phosphatase treatment, Bisgrove *et al.* showed NFI to be hyperphosphorylated in GFAP/B-FABP-negative malignant glioma cell lines compared with GFAP/B-FABP-positive lines.[21] Phosphorylation of NFI did not seem to affect DNA binding activity *in vitro*, in agreement with a previous report.[35] Similarly, transfection and DNase I footprinting analysis revealed three footprints in the promoter region of the *GFAP* gene in the B-FABP/GFAP-positive malignant glioma cell line U251.[36,37] Putative NFI binding sites were identified in all three regulatory regions. Direct evidence demonstrating occupancy of the *GFAP* promoter by NFIs was obtained by chromatin immunoprecipitation (ChIP) using primary cortical neuroepithelial cells.[22]

All four *NFI* genes have been disrupted in mice.[34,38–41] Whereas *Nfic*-deficient animals have defects in tooth root formation, disruption of either *Nfia* or *Nfib* results in forebrain defects and loss of specific midline glial populations. In addition to having more severe forebrain defects than *Nfia*, *Nfib* knock-outs have abnormalities in lung maturation and pons development.[41] *Nfix*−/− mice show enlargement of the lateral and third brain ventricles, expansion of the entire brain along the dorsal ventral axis, aberrant formation of the hippocampus, deformation of the spine, and impaired ossification of vertebra and femur.[39,42] *GFAP* mRNA levels are decreased 10- and 5-fold in *Nfia*−/− and *Nfib*−/− mice, respectively, suggesting involvement of these two NFIs in *GFAP* regulation.[41] Activation of Notch signaling in mid-gestational neural precursor cells has recently been shown to induce NFIA, resulting in demethylation and activation of astrocytic gene promoters including *GFAP*.[43] Thus, NFIA seems to play a fundamental role in potentiating the differentiation of neural precursor cells along the astrocytic lineage.

Here, we investigate the role of NFI in the regulation of the *GFAP* and *B-FABP* genes in malignant glioma cells. We use ChIP to demonstrate the occupancy of NFIs at both the endogenous *GFAP* and the *B-FABP* promoters. We study the expression patterns of all four *NFI* genes in B-FABP/GFAP-positive and B-FABP/GFAP-negative malignant glioma cell lines and use the gel-shift assay to examine the binding of each NFI to three NFI recognition sites located at the 5′ ends of each of the *B-FABP* and *GFAP* genes. We use a combination of RNA interference, ectopic NFI expression, reporter gene assay, and analysis of endogenous *GFAP* and *B-FABP* RNA to investigate the biological activity of NFIs *in vivo*. Our results suggest complex antagonistic and compensatory interactions between the four members of the NFI family, which all seem to be involved in the regulation of *B-FABP* and *GFAP* transcription.

Results

Expression of NFI mRNA in malignant glioma cell lines

The four *NFI* genes (*NFIA*, *NFIB*, *NFIC*, and *NFIX*) are differentially expressed in various tissues and cell types. To identify which NFIs are expressed in malignant glioma cells, Northern blot analysis was carried out using poly(A)$^+$ RNA isolated from five B-FABP/GFAP-negative malignant glioma lines (A172, CLA, M021, T98, and U87) and five B-FABP/GFAP-positive malignant glioma lines (M016, M049, M103, U251, and U373) (Fig. 1). Highest levels of *NFIA* transcripts were detected in M049 and M103. *NFIB* mRNA was most abundant in B-FABP/GFAP-positive M049, M103, U251, and U373 lines. *NFIC* transcripts were found in all 10 lines. Highest levels of *NFIX* mRNA were observed in M103 and M021, with an easily detectable signal in every cell line except U87. Actin mRNA served as the loading control and was relatively uniform in the 10 malignant glioma lines. Overall, B-FABP/GFAP-positive malignant glioma lines seem to express higher levels of NFI mRNAs compared with B-FABP/GFAP-negative lines, with the most dramatic differences observed with *NFIA* and *NFIB*.

In vitro binding of proteins to GFAP NFI recognition sites

Sequence analysis of the *GFAP* promoter region revealed three putative NFI binding sites in the upstream region of the *GFAP* gene, located at −120 to −106 bp, −1585 to −1571 bp, and −1633 to −1619 bp. Each of these three sites is bound by protein based on DNase I footprinting analysis[36,37] and gel-shift assays.[23] We used gel shifts to determine whether NFIs from T98 (B-FABP/GFAP negative) and U251 (B-FABP/GFAP positive) malignant glioma lines could bind to the three putative NFI binding sites located at the 5′ end of the *GFAP* gene. Double-stranded oligonucleotides representing each of the three *GFAP* NFI binding regions [G-br1 (−126 to

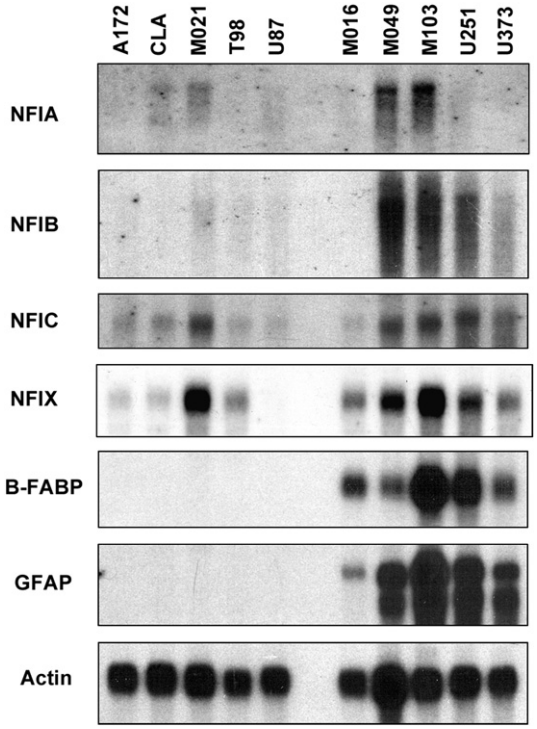

Fig. 1. RNA analysis of malignant glioma cell lines. Northern blots were prepared using poly(A)$^+$ RNA (2 μg per lane) isolated from five human B-FABP/GFAP-negative lines (A172, CLA, M021, T98, and U87) and five human B-FABP/GFAP-positive lines (M016, M049, M103, U251, and U373). The filter was sequentially hybridized with ^{32}P-labeled cDNAs from *NFIA*, *NFIB*, *NFIC*, *NFIX*, *B-FABP*, *GFAP*, and actin.

−100 bp), G-br2 (−1591 to −1564 bp), and G-br3 (−1639 to −1613 bp)] were generated. Radiolabeled oligonucleotides were incubated with nuclear extracts prepared from either T98 or U251 cells. A 100× molar excess of unlabeled competitor oligonucleotides was included in some of the lanes. Competitor oligonucleotides included G-br1, G-br2, G-br3 (wild type and mutated at conserved residues 3 and 4), Sp1, NFI, and AP-2 (activating protein 2) (Fig. 2).

As shown in Fig. 3a, a major DNA–protein complex was observed when G-br1, G-br2, or G-br3 was incubated with T98 nuclear extracts. Addition of excess mutated G-br1*, G-br2*, or G-br3* oligonucleotides as competitors did not result in a significant reduction in the signal intensity of the complex, indicating that protein binding to these oligonucleotides requires an intact NFI binding site. All three unlabeled wild-type G-br oligonucleotides served as effective competitors for all three G-br probes. Furthermore, the intensity of the DNA–protein complex was significantly reduced in the presence of consensus NFI oligonucleotides, but not Sp1 or AP-2 oligonucleotides. These results indicate that the factor bound to G-br1, G-br2, and G-br3 is NFI or NFI-like.

Similar observations were made when G-br1 and G-br2 probes were incubated with U251 nuclear extracts, except that the migration rate of the DNA–protein complex was considerably faster than that observed with T98 extracts (Fig. 3b). These results are in agreement with our previous work indicating that NFIs expressed in U251 and T98 migrate at different rates in gel-shift assays because the T98 NFIs are hyperphosphorylated compared with U251 NFIs.[21] In contrast to G-br1 and G-br2, which generated one major protein–DNA complex, three DNA–protein complexes were observed when U251 nuclear extracts were incubated with G-br3. As the intensity of the middle band (indicated by an arrow) was greatly decreased in the presence of excess wild-type G-br1, G-br2, and G-br3 and NFI consensus oligonucleotides, but not mutated G-br3 oligonucleotide, it is likely that this is the only band that contains NFI–DNA complexes. Interestingly, the faster-migrating complex disappeared in the presence of AP-2 competitor, suggesting the presence of both NFI and AP-2 binding sites within the G-br3 oligonucleotide. Examination of the G-br3 sequence reveals putative AP-2 binding sites (consensus GCCNNNGGC) spanning the NFI binding site.

In vitro binding of proteins to B-FABP NFI recognition sites

Previous work from our laboratory identified two NFI binding sites in the 5′ flanking DNA of the *B-FABP* gene, located at −54 to −40 bp (B-br1) and −256 to −242 bp (B-br3).[21] These sites were identified by DNase I footprinting, and binding of NFI to these sites was confirmed by gel-shift assays and methylation interference. A third putative NFI-like binding site, located at −176 to −163 bp (B-br2), was not analysed because (i) it was found at the 5′ edge of a DNase I footprint and (ii) it had N-4 spacing between the NFI half-sites rather than the consensus N-5 spacing. Addition or subtraction of 1 bp from the 5-bp internal spacer has been shown to drastically reduce NFI binding *in vitro*.[44] We used the gel-shift assay to determine whether a radiolabeled double-stranded oligonucleotide corresponding to B-br2 could bind NFI or NFI-like proteins. As shown in Fig. 4 (left), a DNA–protein complex was observed when U251 nuclear extracts were used, although the intensity of the complex in relation to free oligonucleotides seemed to be low when compared with B-br1 (Fig. 4, right). The protein complex formed with B-br2 was significantly reduced in the presence of excess cold competitors B-br1, B-br2, B-br3, and NFI consensus binding site, but not AP-2 and Sp1 consensus binding sites. Conversely, addition of excess B-br2 significantly reduced the intensity of the DNA–protein complex obtained with B-br1.

In vivo occupancy of NFIs at the endogenous *B-FABP* and *GFAP* promoters

We carried out ChIP analysis using U251 cells and a pan-specific NFI antibody to determine whether NFIs reside in close proximity to *GFAP* and *B-FABP* NFI binding sites *in vivo*. DNA cross-linked to NFIs

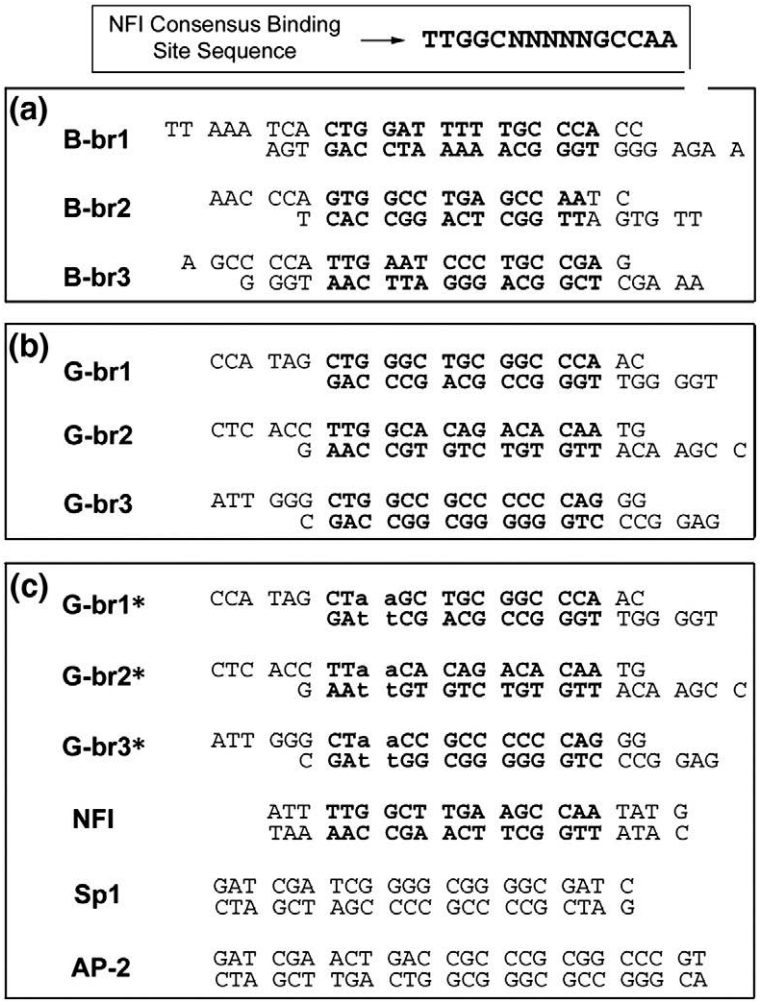

Fig. 2. Oligonucleotides used for the gel-shift experiments. The NFI consensus binding site sequence is indicated on top. The primers used to generate (a) *B-FABP* NFI binding regions (B-br1, B-br2, and B-br3) and (b) *GFAP* NFI binding regions (G-br1, G-br2, and G-br3) are shown with the NFI consensus sites indicated in bold. (c) Site-directed mutagenesis was used to convert the third and fourth residues of the *GFAP* NFI binding regions from GG to AA (indicated in small letters). Both these residues have been shown to be critical for binding to NFI. The sequences of the NFI, Sp1, and AP-2 oligonucleotides are based on consensus binding sites.

was PCR-amplified using primer pairs flanking individual or combined *GFAP* and *B-FABP* NFI binding sites. Normal rabbit IgG served as the negative control for the ChIP experiments. Bands corresponding to each of the three *GFAP* NFI binding sites (G-br1, G-br2, and G-br3) were easily detected using this approach (Fig. 5). Similarly, ChIP analysis revealed NFIs at all three *B-FABP* NFI binding sites, although the intensity of the band obtained with primers flanking B-br1 was weak. No DNA bands were detected in any of the IgG lanes. As well, no signal was detected in either the IgG or the NFI lanes when primers to the *GAPDH* promoter were utilized. Together, these data indicate that NFIs occupy the regions of the *B-FABP* and *GFAP* promoters containing NFI binding sites.

Binding of specific NFIs to GFAP and B-FABP NFI recognition sites

Our gel-shift data suggest that one or more NFI proteins can bind to each of the three NFI recognition sites located upstream of the *GFAP* gene (Fig. 3) as well as to the three NFI recognition sites located upstream of the *B-FABP* gene (Fig. 4).[21] To address the specificity of the different NFI proteins for *GFAP* and *B-FABP* NFI recognition sites, we examined the binding of each of the four NFIs to G-br and B-br oligonucleotides. T98 cells were transfected with hemagglutinin (HA)-tagged NFIA, NFIB, NFIC, and NFIX expression constructs as well as empty vector. Nuclear extracts were prepared and analysed for the level of NFI protein. As shown in Fig. 6a, each HA-tagged NFI protein was abundantly expressed in T98 transfectants, with NFIA present at ~2-fold lower levels and NFIC expressed at ~1.5-fold higher levels compared with NFIB and NFIX.

For the gel-shift assays, an equal amount of each of these nuclear extracts (~1 μg of protein) was incubated with radiolabeled G-br1, G-br2, and G-br3 oligonucleotides (Fig. 6b). Strong binding was observed when either NFIA or NFIX was incubated with G-br1, whereas NFIB and NFIC generated weaker signals. Similarly, a strong signal was observed when NFIX was incubated with G-br3, with a weaker signal observed with NFIA. There was no apparent change in signal intensity in lanes containing NFIB and NFIC compared with pCH control. In contrast to G-br1 and G-br3, all four NFIs generated a strong signal when incubated with G-br2. Addition of anti-HA antibody to NFIX-enriched nuclear extracts resulted in a supershifted band (arrowhead), indicating that HA-NFIX binds to G-Br2. The residual band in this lane is of the same

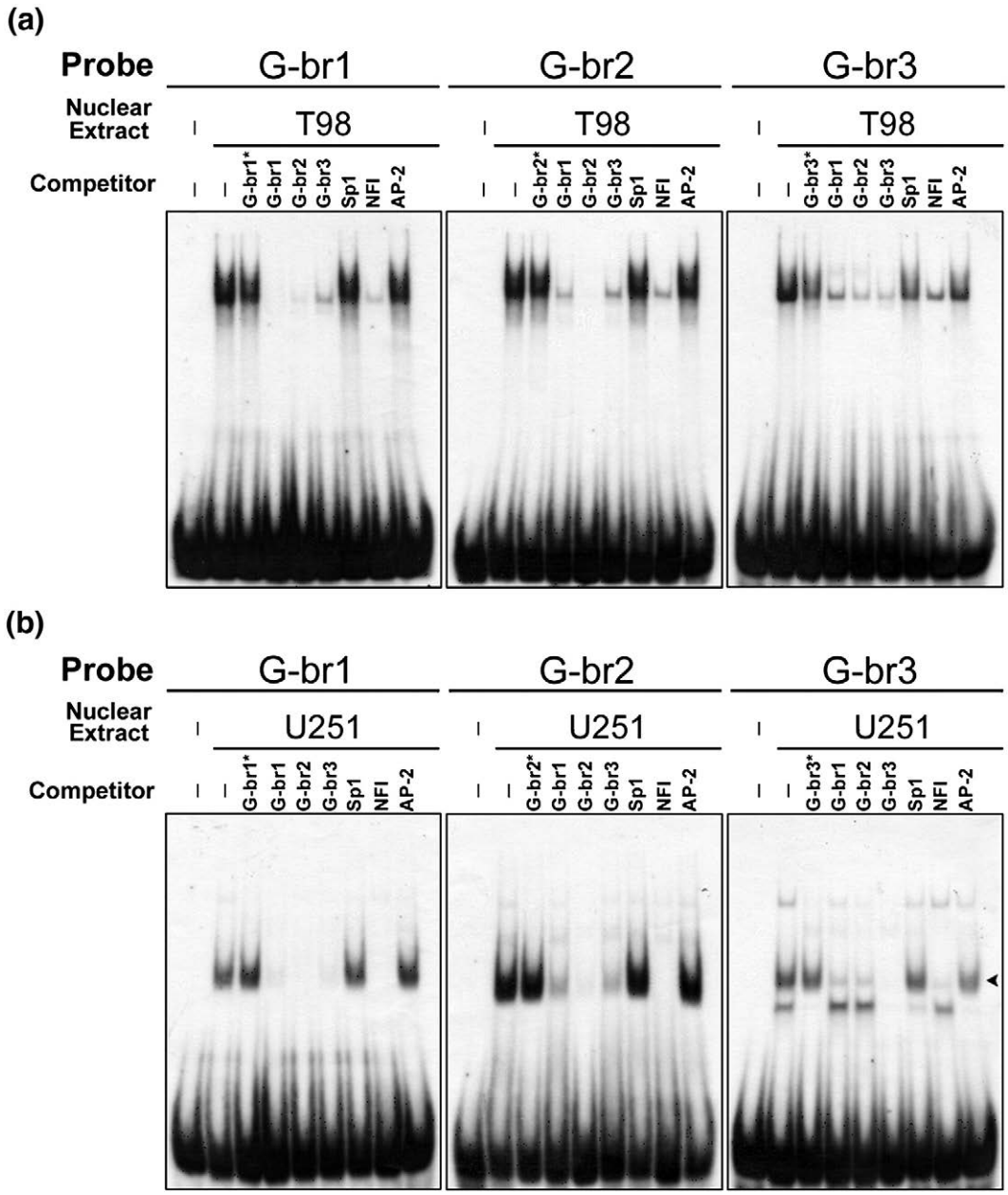

Fig. 3. Binding of NFI to G-br1, G-br2, and G-br3. Gel-shift experiments were carried out with radiolabeled G-br1, G-br2, or G-br3 double-stranded oligonucleotides and (a) T98 or (b) U251 nuclear extracts. DNA binding reactions were electrophoresed in a 6% polyacrylamide gel in 0.5× TBE buffer to separate unbound DNA and DNA–protein complexes. Where indicated, a 100-fold excess of unlabeled competitor oligonucleotides was added to the DNA binding reaction. The asterisks indicate that the NFI binding site was mutated.

intensity as that seen in pCH control and likely represents endogenous NFIs binding to G-br2.

To address whether the shifted band observed in the pCH (control) lanes represents endogenous NFI bound to G-br oligonucleotides, we carried out supershift experiments with an anti-NFI antibody previously used to supershift the endogenous NFI–B-br1 complex.[21] This antibody preferentially recognizes NFIC, although it can also bind to NFIX (data not shown). Addition of anti-NFI antibody to G-br2 oligonucleotides in the presence of nuclear extracts derived from pCH-transfected T98 cells produced a supershifted band (shown by arrow), indicating the presence of an anti-NFI antibody–NFI protein–G-br2 oligonucleotide tri-complex (Fig. 6c). The weak intensity of the supershifted band combined with the decrease in intensity of the shifted band indicates that the anti-NFI antibody used in these experiments interferes with the binding of the transcription factor to G-br2. As expected, neither anti-AP-2 antibody nor anti-Pax6 antibody produced a supershifted band or affected NFI binding to G-br2.

Next, we examined binding of the four NFIs to labeled oligonucleotides corresponding to the three NFI-like binding sites in the upstream region of the *B-FABP* gene. Gel-shift assays indicated that all four

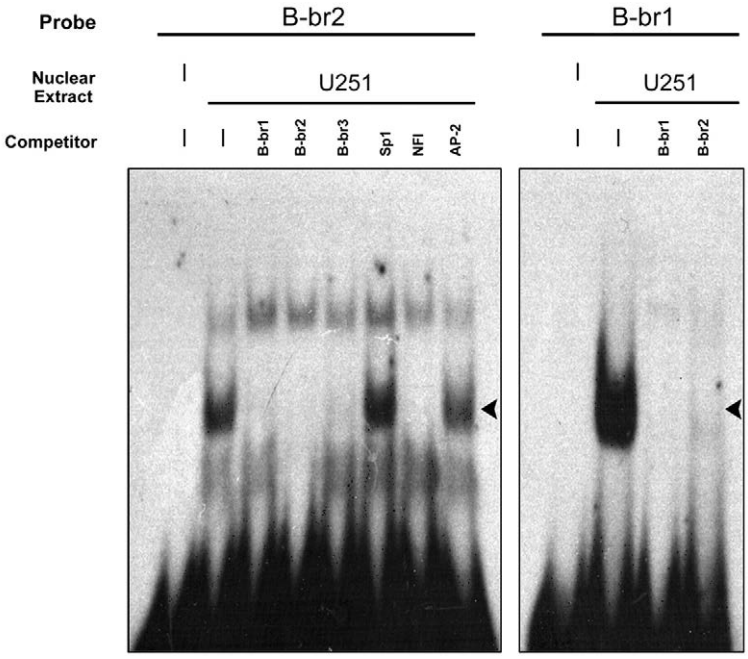

Fig. 4. Binding of NFI to B-br2. Gel-shift experiments were carried out with radiolabeled B-br2 double-stranded oligonucleotide. The arrowhead indicates the protein–DNA complex specific to B-br2 (left) and B-br1 (right).

NFI proteins could effectively bind B-br1 and B-br2 (Fig. 6d), although NFIC and NFIX generated a stronger signal than did NFIA and NFIB when incubated with B-br1. The most striking differential binding was observed when B-br3 oligonucleotide was used as the probe, with NFIX producing the strongest signal, followed by NFIC, then NFIA. Incubation of B-br3 with nuclear extracts from NFIB-transfected cells produced only background signal. Combined, our results suggest that specific NFIs (alone or in combination with other proteins found in the nuclear extracts) preferentially bind to specific NFI recognition sites.

Transcriptional regulation of GFAP and B-FABP by NFI proteins

To study the role of the different members of the NFI family in the regulation of *B-FABP* and *GFAP* promoter activity *in vivo*, U251 cells were co-transfected with (i) plasmids containing the chloramphenicol acetyltransferase (CAT) reporter gene under the control of either the *GFAP* (pCAT/GFAP-1708) or the *B-FABP* (pCAT/B-FABP-1785) upstream region and (ii) NFI expression constructs. Ectopic expression of NFIA had the strongest effect on the *GFAP* promoter, increasing CAT activity by 5.4-fold compared with cells transfected with pCH control vector (Fig. 7a). In comparison, NFIB, NFIC, and NFIX expression constructs increased GFAP-driven CAT activity by 2.9-, 2.1-, and 2.7-fold, respectively. In contrast, ectopic expression of either NFIC or NFIX resulted in a 2.2- and 1.9-fold reduction in *B-FABP* promoter activity, respectively (Fig. 7b). No differences in CAT activity were observed in cells co-transfected with pCAT/B-FABP-1785 and either the NFIA or NFIB expression construct.

The β-galactosidase expression construct under the control of the SV40 promoter was initially used to control for plate-to-plate variation in transfection efficiency. However, the SV40 promoter was found to be highly responsive to NFIC. To preclude any modifying effect of NFIs on control reporter genes, we used Southern blotting of nonintegrated (Hirt) DNA to control for transfection efficiency.[45] As shown in Fig. 7c, there was little variation in the level of nonintegrated plasmid DNA within each set of transfected cells. Thus, the CAT activity shown in Fig. 7a and b is a direct measurement [in counts per minute (cpm)] of acetylated [^{14}C]chloramphenicol,

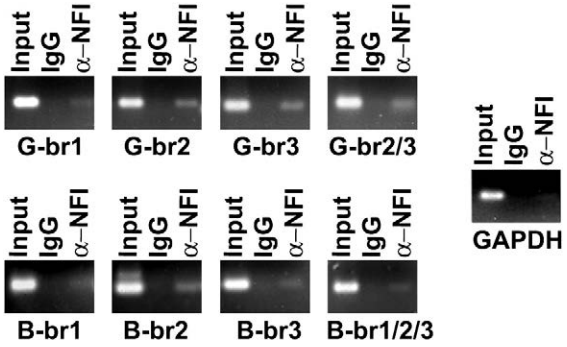

Fig. 5. ChIP analysis indicating that NFIs occupy the endogenous *GFAP* and *B-FABP* promoters. ChIP analyses were carried out using either a pan-specific anti-NFI antibody or normal rabbit IgG and U251 cell lysates. Primers flanking the NFI recognition sites identified in the *GFAP* and *B-FABP* promoters (G-br1, G-br2, G-br3, G-br2/3, B-br1, B-br2, B-br3, and B-br1/2/3) were used for PCR amplification. Primers corresponding to the proximal *GAPDH* promoter (200-bp upstream region) were used as a negative control. Input DNA represents DNA isolated from U251 cell lysates after sonication but prior to immunoprecipitation. Input DNA reveals PCR-amplified products of the expected sizes for all primer combinations analysed.

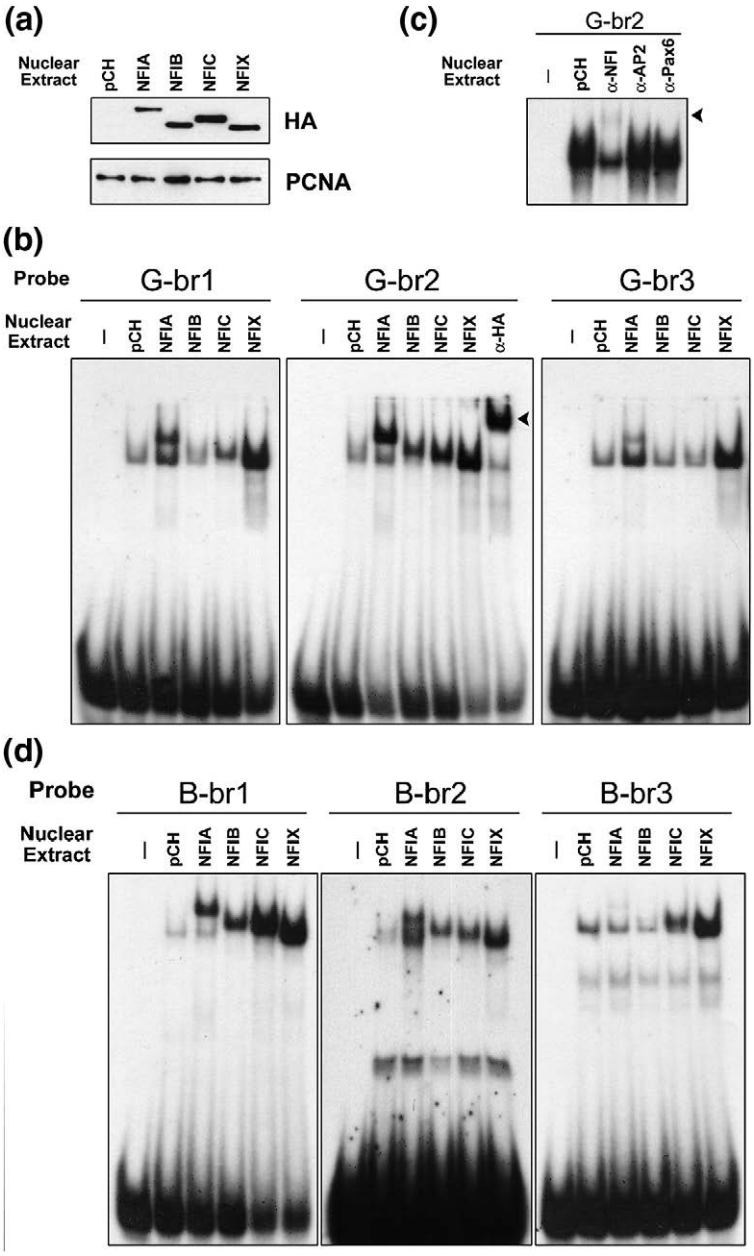

Fig. 6. Binding of NFIA, NFIB, NFIC, and NFIX to *GFAP* and *B-FABP* NFI recognition sites. Nuclear extracts were prepared from T98 cells transfected with control (pCH), pCHNFIA, pCHNFIB, pCHNFIC, or pCHNFIX expression constructs. (a) Western blot analysis of transfected cells. Nuclear extracts (10 μg per lane) were electrophoresed through a 10% polyacrylamide–SDS gel and electroblotted onto a nitrocellulose filter. The filter was incubated with mouse anti-HA antibody or mouse anti-proliferating cell nuclear antigen antibody, and the signal was detected using the ECL system. (b) Gel-shift experiments were carried out using radiolabeled G-br1, G-br2, or G-br3 and 1 μg of nuclear extract. A supershift experiment (labeled α-HA; middle) was performed by incubating anti-HA antibody with nuclear extracts prepared from T98 cells transfected with NFIX. The arrowhead shows the supershifted band. (c) Supershift experiment using radiolabeled G-br2, 1 μg of nuclear extract from T98 transfected with pCH vector, and anti-NFI, anti-AP-2, or anti-Pax6 antibody. The arrowhead indicates the position of the supershifted band. (d) Gel-shift experiments were carried out using radiolabeled B-br1, B-br2, or B-br3 and 1 μg of nuclear extract.

with cpm values obtained for each of the pCH/NFI expression constructs compared with pCH control.

To determine whether overexpression of NFIs affects endogenous GFAP and B-FABP protein levels, we carried out Western blot analysis of U251 cells transfected with individual NFI expression constructs. Although high levels of HA-tagged NFI proteins were observed in transfected cells, there were no significant differences in GFAP and B-FABP levels compared with controls (Fig. 7d). These results indicate that factors in addition to NFI are required for regulation of endogenous B-FABP and GFAP expression.

The role of NFIs in the regulation of *GFAP* and *B-FABP* transcription was further investigated with the use of an RNA interference approach to reduce endogenous levels of specific NFIs in U251. Cells were first transfected with control (scrambled) small interfering RNA (siRNA) or siRNAs targeting *NFIA*, *NFIB*, *NFIC*, or *NFIX* under conditions that resulted in ~90% transfection efficiency. Twenty-four hours later, the same cultures were transfected with either pCAT/GFAP-1708 or pCAT-B-FABP-1785. Cells were harvested 60 h after the second transfection and analysed for (i) endogenous *NFIA*, *NFIB*, *NFIC*, and *NFIX* RNA levels (Fig. 8a); (ii) endogenous *GFAP* and *B-FABP* RNA levels (Fig. 8b); and (iii) pCAT activity (Fig. 8c). Real-time quantitative reverse transcription-PCR (RT-PCR) analysis revealed 79% or greater reduction in *NFIA*, *NFIB*, *NFIC*, and *NFIX* RNA levels in NFI siRNA-transfected cells compared with control siRNA-transfected cells. Two separate experiments are represented in Fig. 8a, with pCAT/GFAP-1708 co-transfectants shown on the left and pCAT/B-FABP-1785 co-transfectants shown on the right. Interest-

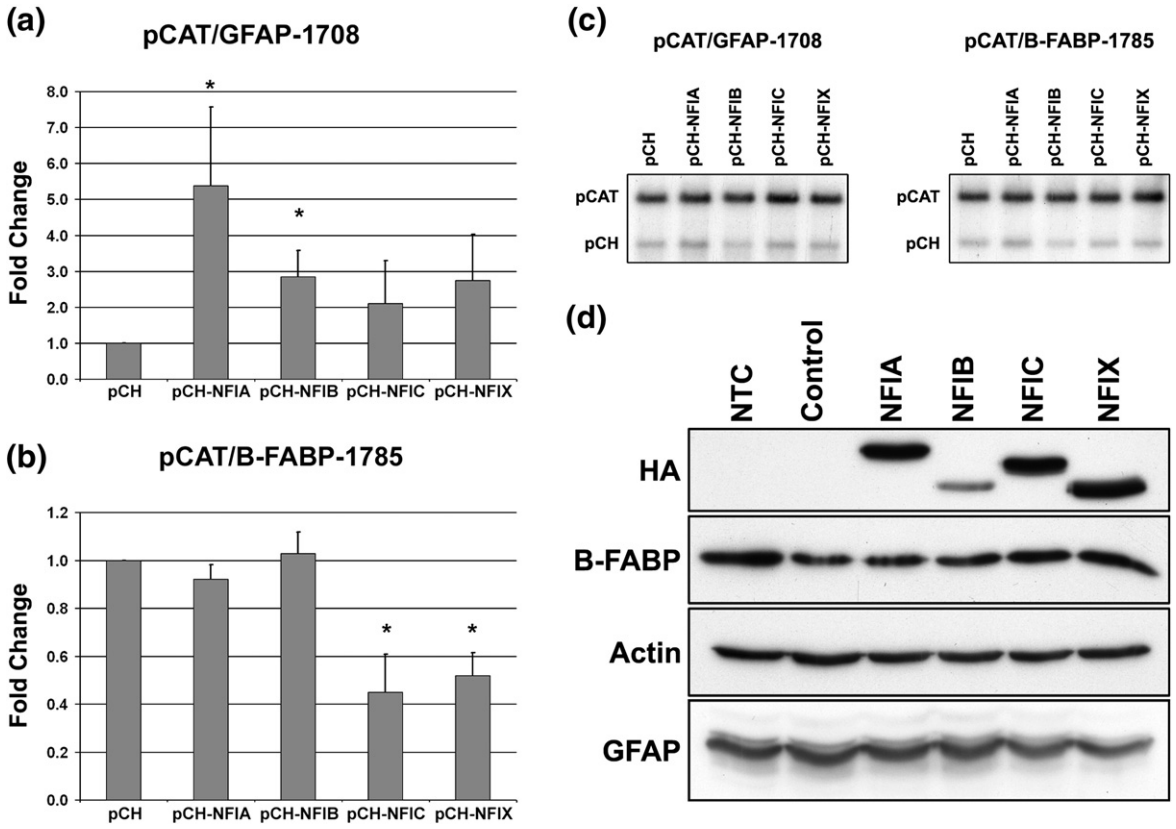

Fig. 7. Co-transfection of NFI expression constructs with pCAT/GFAP or pCAT/B-FABP reporter genes. U251 cells were co-transfected with pCAT/GFAP-1708 (a) or pCAT/B-FABP-1785 (b) and pCH/NFI expression constructs. Acetylated [^{14}C]chloramphenicol was measured (in cpm) from equal aliquots of transfected cell lysates using a scintillation counter. The fold increases in CAT activity are relative to the pCH (empty vector) co-transfectants. The ratio of pCAT plasmid DNA to pCH/NFI expression construct was 10:1 (i.e., 3.6 μg of pCAT plasmid DNA and 0.4 μg of pCH/NFI expression construct per 60-mm plate). The results shown are an average of three to five independent experiments with SEM indicated by the error bars. Statistical significance was determined using the unpaired *t* test. The asterisk indicates that the data are significantly different from that of the pCH control ($P<0.05$). (c) Southern blot analysis of nonintegrated (Hirt) DNA from two representative experiments. Hirt DNA was extracted from the same fraction (typically 1/5 or 1/4) of cells from each plate. Equal aliquots of DNA were digested with BamH1, electrophoresed on a 1% agarose gel, transferred onto nitrocellulose, and probed with ^{32}P-labeled pCAT-basic vector DNA. The top band represents the pCAT/GFAP-1708 DNA (left) and pCAT/GFAP-1785 DNA (right). The lower-migrating band represents the co-transfected pCH/NFI–DNA. As shown here, there was little variation in amount of transfected DNA from plate to plate. (d) Western blot analysis of B-FABP and GFAP in U251 cells overexpressing NFIs. U251 cells were transfected with individual pCH/NFI expression constructs (4–8 μg per 100-mm plate) and cells were harvested 60 h later. Cell lysates (50 μg/lane) were electrophoresed in a 13.5% acrylamide–SDS gel (HA, B-FABP, and actin) or 10% acrylamide–SDS gel (GFAP), transferred onto PVDF membranes, and immunostained with mouse anti-HA antibody, rabbit anti-B-FABP antibody, and mouse anti-actin antibody (13.5% gel) and mouse anti-GFAP antibody (10%). Primary antibodies were detected with horseradish-peroxidase-conjugated secondary antibodies and the signal was detected using the ECL reagent. Because levels of HA-tagged NFIB were consistently lower than those of the other NFIs, we transfected cells with a range of pCH/NFIB DNA (0.8–16 μg per 100-mm plate). HA-NFIB levels increased up to 8 μg of transfected DNA and remained constant from 8 to 16 μg of transfected DNA, suggesting posttranslational regulation of NFIB protein levels in U251 cells.

ingly, reduction of one NFI often resulted in up-regulation of a second NFI, suggesting cross talk between the different members of the NFI family. For example, NFIA knock-down resulted in increased *NFIX* RNA levels, NFIB knock-down increased *NFIA* RNA levels, NFIC knock-down decreased *NFIB* RNA levels, whereas NFIX knock-down cells showed increased levels of *NFIA* RNA.

Next, we examined endogenous *GFAP* and *B-FABP* RNA levels in NFI knock-down cells by real-time RT-PCR. The most consistent and dramatic decreases in endogenous *GFAP* RNA levels were observed in cells transfected with *NFIB* and *NFIC* siRNAs, followed by *NFIX* and *NFIA* siRNAs (Fig. 8b, top). There was a slight (10–40% depending on the experiment) reduction in endogenous *B-FABP* RNA levels in cells transfected with *NFIA* siRNA, indicating that NFIA may play a positive role in *B-FABP* transcription. A 1.6- to 2-fold increase in *B-FABP* RNA was consistently observed in NFIB knock-down cells (Fig. 8b, bottom). These data suggest either that NFIB functions as a repressor of endogenous *B-FABP*

promoter activity or, more likely in light of the elevated endogenous *NFIB* RNA levels observed in B-FABP-positive glioma cells, that the increase in *NFIA* RNA levels associated with NFIB knock-down activates the *B-FABP* promoter.

As promoter analyses are classically carried out using reporter genes, we also used the CAT reporter gene under the control of the 1.7- or 1.8-kb *GFAP* or *B-FABP* promoter, respectively, to investigate the effect of NFI knock-down on transcriptional activity. Analysis of CAT activity in U251 cells co-transfected with pCAT/GFAP-1708 and NFI siRNAs revealed decreased transcriptional activity in NFIA (37% of control), NFIB (50%), and NFIX (48%) knock-downs (Fig. 8c), suggesting a positive role for these three NFIs in *GFAP* regulation. Surprisingly, CAT activity was increased 2.3-fold in NFIC knock-downs even though endogenous *GFAP* RNA levels were significantly reduced in these cells. Similar to pCAT/GFAP transfectants, decreases in CAT activity were observed in cells co-transfected with pCAT/B-FABP-1785 and either *NFIA* or *NFIB* siRNAs (Fig. 8c), in support of a positive role for these two NFIs in *B-FABP* regulation. NFIC seems to play a major repressor role in *B-FABP* transcription, as cells co-transfected with *NFIC* siRNA showed a 15-fold increase in *B-FABP* promoter activity. As mentioned earlier, endogenous *B-FABP* RNA levels were not altered upon *NFIC* knock-down (Fig. 8b). These results suggest a fundamental difference in the way that the NFIC transcription factor interacts with chromosomal *versus* episomal *B-FABP* and *GFAP* NFI binding sites.

To investigate whether decreases in endogenous *GFAP* RNA were accompanied by decreases in GFAP protein levels, we transfected U251 cells with control siRNA or individual siRNAs targeting each of the four NFIs. No decreases in GFAP protein levels were observed 60 h after the initial transfection. However, significant decreases in GFAP were observed after a second round of transfection with *NFIB*, *NFIC*, or *NFIX*, but not *NFIA*, siRNAs (Fig. 9a). After a total of three consecutive transfections, GFAP was barely detectable in *NFIB*, *NFIC*, and *NFIX* siRNA transfectants and dramatically reduced in *NFIA* siRNA transfectants. No alterations in B-FABP protein levels were observed in U251 cells transfected once with NFI siRNAs. After two rounds of transfections, a slight increase in B-FABP was observed in the NFIB knock-down cells, in agreement with the RNA data (Figs. 9b and 8b). An ~2–4-fold decrease in B-FABP levels was observed in all four NFI knock-downs after three consecutive rounds of transfections, with the greatest reduction observed in cells transfected with *NFIX* siRNA. Because of the lag time, it is not clear whether the reduction in B-FABP levels observed after three rounds of transfection is a direct or indirect consequence of NFI knock-down.

Overall, there was general agreement between the NFI overexpression and knock-down data with regard to GFAP. Overexpression of all four NFIs increased ectopic *GFAP* promoter activity, whereas reduction in the levels of all four NFIs decreased endogenous *GFAP* RNA (and eventually protein) levels. Furthermore, ectopic *GFAP* promoter activity was decreased upon NFIA, NFIB, and NFIX knock-down. The situation with B-FABP seems to be considerably more complex as NFI overexpression either had no effect (NFIA and NFIB) or resulted in decreased ectopic *B-FABP* promoter activity (NFIC and NFIX). Reduction in NFI levels was accompanied by increased endogenous *B-FABP* mRNA in the case of NFIB, decreased B-FABP protein levels after multiple rounds of transfection, and either decreased (NFIA and NFIB) or dramatically increased (NFIC) ectopic *B-FABP* promoter activity.

Mutational analysis of NFI binding sites in the GFAP promoter

We have previously shown that mutation of NFI binding sites in the *B-FABP* promoter reduces its transcriptional activity.[21] Here, we extend the analysis to *GFAP* by mutating the NFI recognition sites in the *GFAP* upstream region (Fig. 10a), first in the context of the pCAT/GFAP-168 construct, which contains the G-br1 binding site, and second in the context of pCAT/GFAP-1705, which contains all three NFI binding sites.

As shown in Fig. 10b, a 3.2-fold increase in CAT activity was observed with wild-type pCAT/GFAP-168 compared with pCAT basic vector. To investigate which of the four NFIs target G-br1, pCAT/GFAP-168 was co-transfected into U251 cells along with control or NFI siRNAs. Decreased CAT activity was observed in the presence of *NFIB* siRNA and increased CAT activity in the presence of *NFIC* siRNA, indicating that at least these two NFIs bind to G-br1 (Fig. 10c). In this regard, it is interesting to note that NFIB and NFIC showed the weakest binding to G-br1 based on the gel-shift assay (Fig. 6b). Mutation of G-br1 in pCAT/GFAP-168 completely abolished its transcriptional activity, with no further decreases observed upon co-transfection of NFI siRNAs (Fig. 10b and c).

CAT activity was induced 7.6-fold in pCAT/GFAP-1708-transfected cells compared with pCAT basic vector (Fig. 10b). Mutation in G-br1* resulted in a 5.1-fold decrease in CAT activity (1.5-fold increase compared with pCAT basic), mutation in combined G-br2*/G-br3* resulted in a 2.2-fold decrease in CAT activity (3.4-fold increase compared with pCAT basic), whereas combined mutation of G-br1*/G-br2*/G-br3* reduced CAT activity 6-fold (1.3-fold increase compared with pCAT basic), thus demonstrating the importance of the NFI binding sites, particularly G-br1, in the *GFAP* promoter. Although overall CAT activity was barely above background in pCAT/GFAP-1708 G-br1*-transfected cells, knock-down experiments revealed a 2.9-fold increase in CAT activity in the presence of *NFIC* siRNA, suggesting that NFIC can still interact with G-br2 and G-br3 in the absence of G-br1. Knock-down of NFIA in pCAT/GFAP-1708 G-br2*/G-br3*-transfected cells produced the most dramatic

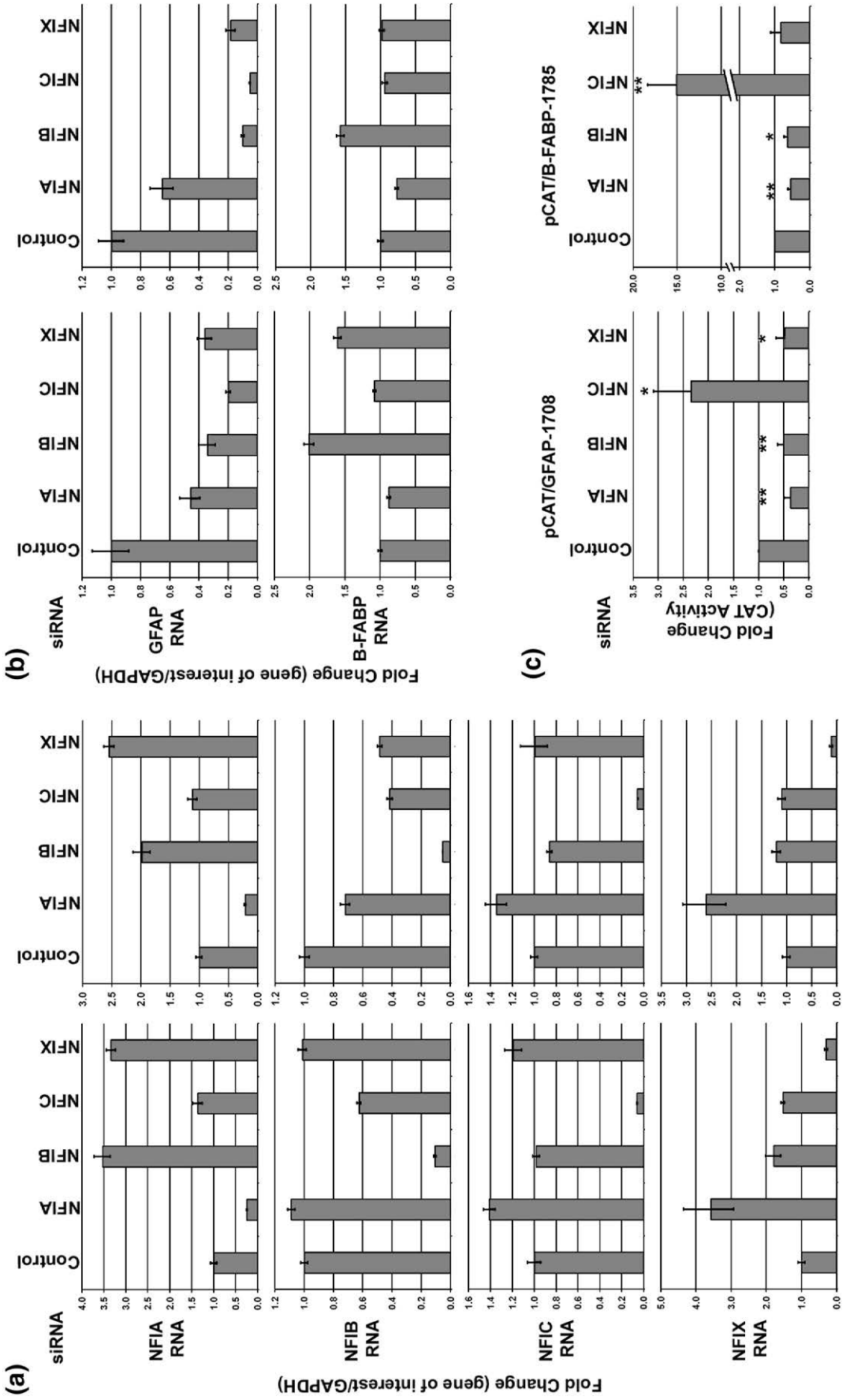

Fig. 8 *(legend on next page)*

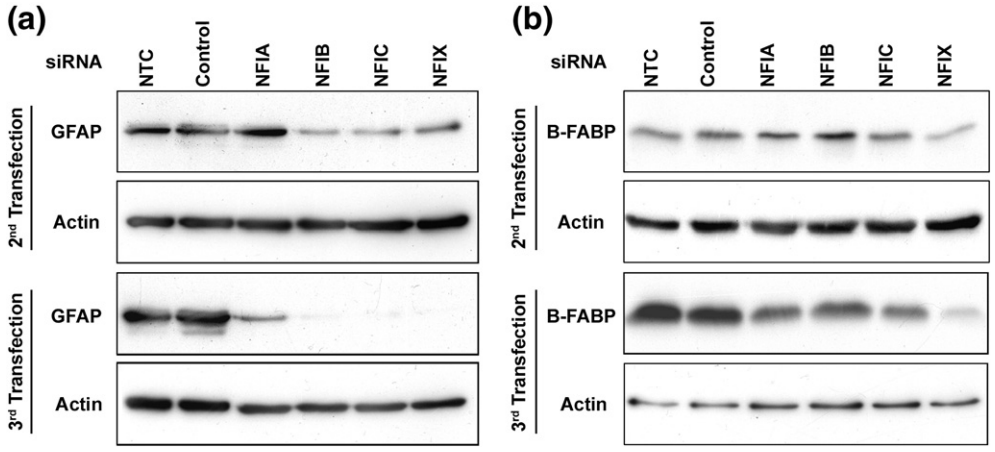

Fig. 9. Western blot analysis of B-FABP and GFAP in U251 cells transiently transfected with NFI siRNAs. U251 cells were sequentially transfected three times with 10 nM control, *NFIA*, *NFIB*, *NFIC*, and *NFIX* Stealth siRNAs over a period of 12 to 15 days. Cells were harvested after each transfection and whole-cell lysates were prepared. For the second and third rounds of transfection, 1/10 of the cells were replated and retransfected and allowed to reach confluence prior to harvest (and replating). Cell lysates (40 μg per lane) were electrophoresed, transferred onto PVDF membranes, and immunostained with (a) mouse anti-GFAP and (b) rabbit anti-B-FABP antibodies. Membranes were then stripped and probed with mouse anti-actin antibody. Primary antibodies were detected with horseradish-peroxidase-conjugated secondary antibodies and the signal was detected using the ECL reagent. No changes in GFAP and B-FABP levels were observed after the first transfection (data not shown). NTC, non-transfected control.

decrease in CAT activity. As expected, only minor variations compared with basal CAT activity were observed in cells transfected with the triple-mutant construct. These results indicate that G-br1 plays a major role in *GFAP* regulation, although it is clear that G-br2 and G-br3 are also involved in this process. Mutation analysis in the context of the *GFAP-1708* promoter suggests a positive regulatory role for NFIA primarily through G-br1 and an inhibitory role for NFIC primarily through G-br2 and G-br3.

Combined NFI knock-downs reveal cross talk between all four members of the NFI family

As shown earlier, knock-down of one NFI can affect the levels of other NFIs, suggesting cross talk between different members of the NFI family. To further investigate the possibility of cross talk or compensatory feedback loops within the NFI family, we transfected U251 cells with the following combinations of NFI siRNAs: NFIA/NFIB, NFIC/NFIX, NFIA/NFIB/NFIC, NFIA/NFB/NFIX, and NFIA/NFIB/NFIC/NFIX (Fig. 11). For these experiments, the total concentration of siRNA used per plate ranged from 10 nM for single transfectants (NFIA) to 40 nM for quadruple siRNA transfectants (NFIA/NFIB/NFIC/NFIX). As shown in Supplementary Fig. 1, similar results were obtained for the quadruple knock-downs when the total amount of siRNA transfected per plate was 10 nM.

Transfection of combined *NFIA/NFIB* siRNAs resulted in increased *GFAP* promoter activity compared with *NFIA* siRNA alone (Fig. 11a). There was a 1.5-fold increase in CAT activity in cells transfected with combined *NFIC/NFIX* siRNAs, whereas combined *NFIA/NFIB/NFIC* siRNAs generated close to control levels of CAT activity. Knock-down of all four NFIs resulted in a 60% decrease in CAT activity compared with control transfectants. These data support a role for all four NFIs in episomal *GFAP* regulation and also indicate that the ratio of the four NFIs may be an important determinant of *GFAP* transcriptional activity, thus explaining the "normalization" of *GFAP* promoter activity observed upon transfection of multiple NFI siRNAs.

Fig. 8. Regulation of *B-FABP* and *GFAP* promoter activity by NFIs. U251 cells were transfected with 10 nM control (scrambled), *NFIA*, *NFIB*, *NFIC*, or *NFIX* Stealth siRNAs, followed by pCAT/GFAP-1708 or pCAT/B-FABP-1785 (4 μg per 60-mm plates) 24 h later. Cells were harvested after an additional 60 h. (a) Quantitative RT-PCR analysis of *NFIA*, *NFIB*, *NFIC*, and *NFIX* in two representative experiments, with pCAT/GFAP-1708 co-transfectants shown on the left and pCAT/B-FABP-1785 co-transfectants shown on the right. The fold changes in endogenous *NFIA*, *NFIB*, *NFIC*, and *NFIX* RNA levels (*y*-axis) are shown for each of the control, *NFIA*, *NFIB*, *NFIC*, and *NFIX* siRNA transfectants (indicated on the *x*-axis). (b) Quantitative RT-PCR analysis of endogenous *GFAP* and *B-FABP* RNA levels in the two sets of transfectants described in (a). *GAPDH* served as the standard for the quantitative RT-PCR analysis. Similar data were obtained in four separate experiments. (c) CAT activity in U251 cells transiently transfected with siRNAs and pCAT vectors, as described in (a). Changes in CAT activity are relative to the CAT activity obtained in cells co-transfected with control siRNA and either pCAT/GFAP-1708 or pCAT/B-FABP-1785. The data are from three independent experiments, each carried out in duplicate. SEM is indicated by the error bars. Statistical significance, determined using the unpaired *t* test, is indicated by one asterisk ($P<0.05$) or two asterisks ($P<0.001$).

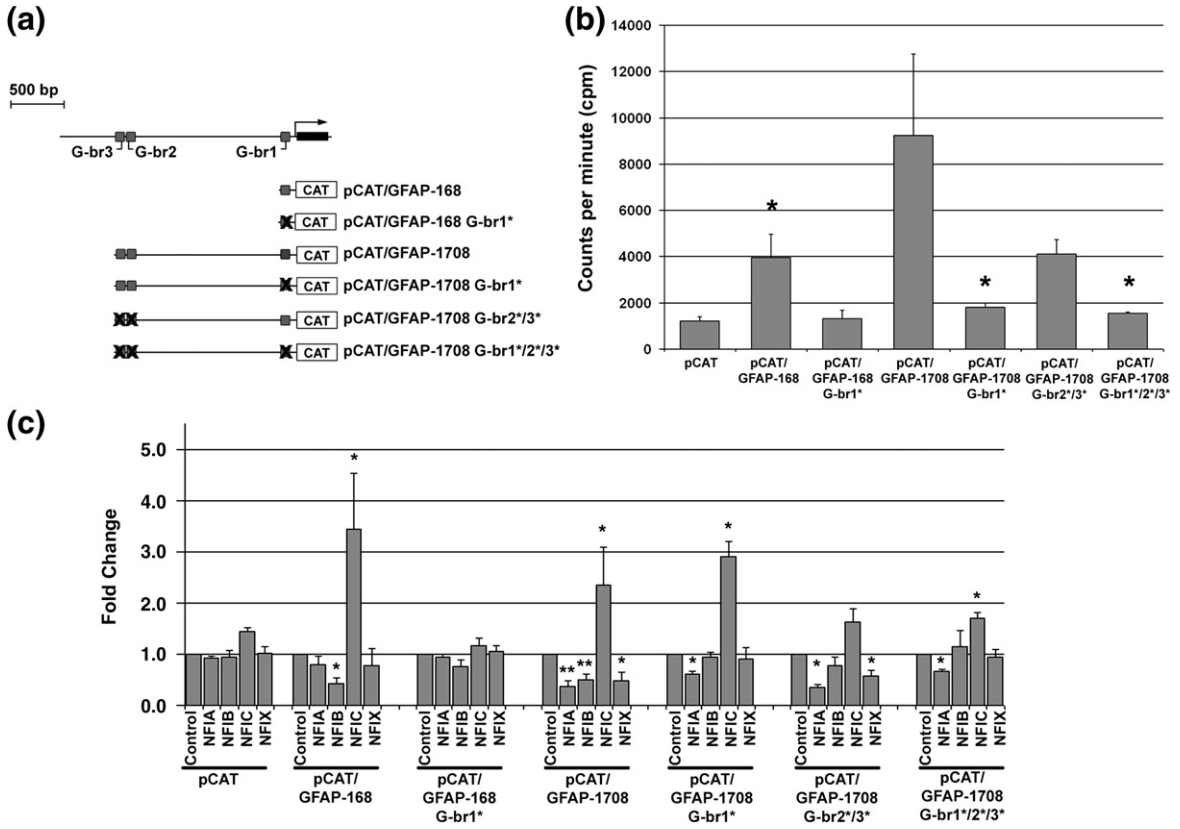

Fig. 10. Mutational analysis of NFI binding sites in the *GFAP* promoter. (a) Schematic diagram of the *GFAP* promoter region showing the relative location of the three NFI binding sites and the names of the wild-type (pCAT/GFAP-168 and pCAT/GFAP-1708 carrying 168 and 1708 of 5′ flanking DNA, respectively) and mutant (pCAT/GFAP-168 G-br1* with mutated G-br1, pCAT/GFAP-1708 G-br1*, pCAT/GFAP-1708 G-br2*/3* with mutated G-br2 and G-br3, and pCAT/GFAP-1708 G-br1*/2*/3* mutated at all three NFI recognition sites) constructs. The transcription start site is indicated by the arrow. (b) CAT activity (in cpm) obtained upon transfection of U251 cells with each of the wild-type and mutant constructs indicated in (a) as well as pCAT basic (containing neither promoter nor enhancer). Four micrograms of DNA was used to transfect each 60-mm plate. (c) Relative CAT activity obtained from U251 cells transfected with 10 nM control, *NFIA*, *NFIB*, *NFIC*, or *NFIX* siRNA, followed 24 h later by transfection with the indicated CAT reporter constructs (4 μg per 60-mm plate). Changes in CAT activity are relative to the CAT activity obtained in cells co-transfected with the indicated pCAT construct and control siRNA. The data are from three independent experiments, each carried out in duplicate. SEM is indicated by the error bars. Statistical significance, determined using the unpaired *t* test, is indicated by one asterisk ($P<0.05$) or two asterisks ($P<0.001$).

In contrast to the *GFAP* promoter, knock-down of combined NFIA/NFIB in pCAT/B-FABP-1785 transfectants resulted in a cumulative decrease in *B-FABP* promoter activity [to background levels (or 27% of the levels observed with scrambled siRNA) and 48% of levels observed with *NFIA* siRNA] (Fig. 11b). These results suggest an important role for both NFIA and NFIB in *B-FABP* transcription. It is noteworthy that in spite of targeting all three positive-acting NFIs while retaining the inhibitory NFIC, the *NFIA/NFIB/NFIX* siRNA combination did not result in a further decrease in CAT activity compared with the NFIA knock-down. Inclusion of *NFIC* siRNA in any combination of NFI siRNAs (*NFIC/NFIX*, *NFIA/NFIB/NFIC*, or *NFIA/NFIB/NFIC/NFIX*) increased *B-FABP* promoter activity, although the fold increase in CAT activity was lower than that obtained with *NFIC* siRNA alone (Fig. 8) and a significant increase was observed only with the *NFIC/NFIX* siRNA combination (Fig. 11b). The quenching effect observed upon transfection of *NFIX* siRNA along with *NFIC* siRNA (compared with *NFIC* siRNA alone) suggests a positive role for NFIX in *B-FABP* promoter activity, even though single NFIX knock-down has little effect on this promoter. Cultures transfected with all four NFI siRNAs still showed a 2-fold increase in CAT activity compared with control transfectants, demonstrating the complex interplay between the positive-acting and negative-acting NFIs.

We then investigated how knock-down of combined NFIs might affect endogenous *GFAP* and *B-FABP* RNA levels. In agreement with the single NFI knock-down data indicating roles for all four NFIs in endogenous *GFAP* regulation (Figs. 8 and 9), all combinations of NFI siRNAs tested generated significant decreases in endogenous *GFAP* levels. The most significant reductions in *GFAP* RNA were observed when *NFIC* siRNA was included in the siRNA mixes, as predicted by the single *NFIC*

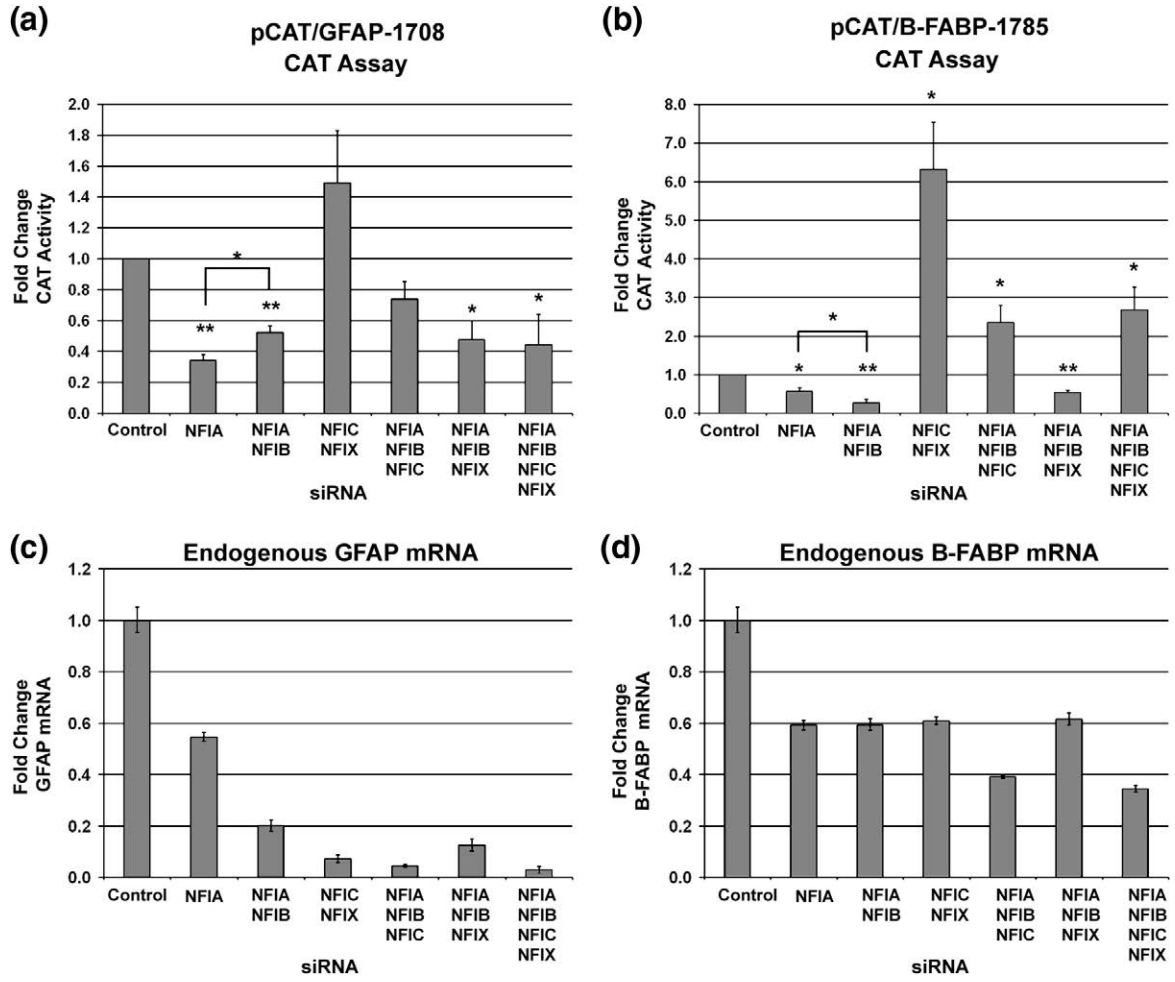

Fig. 11. Regulation of episomal and endogenous *GFAP* and *B-FABP* promoter activity by combined NFI knock-downs. U251 cells were transfected with control (scrambled), *NFIA*, *NFIA/NFIB*, *NFIC/NFIX*, *NFIA/NFIB/NFIC*, *NFIA/NFIB/NFIX*, or *NFIA/NFIB/NFIC/NFIX* Stealth siRNAs (10 nM for each siRNA). (a and b) Twenty-four hours after siRNA transfection, cells were transfected with pCAT/GFAP-1708 (a) or pCAT/B-FABP-1785 (b) (4 μg per 60-mm plate). Cells were harvested after an additional 60 h, then lysed and assayed for CAT activity. Changes in CAT activity are relative to the CAT activity obtained in cells co-transfected with control siRNA and either pCAT/GFAP-1708 or pCAT/B-FABP-1785. The data are from three independent experiments. SEM is indicated by the error bars. Statistical significance, determined by the unpaired *t* test, is indicated by one asterisk ($P<0.05$) or two asterisks ($P<0.001$). (c and d) Quantitative RT-PCR analysis of endogenous *GFAP* (c) and *B-FABP* (d) RNA in U251 cells transfected with NFI siRNAs. Cells were harvested 60 h after transfection. *GAPDH* served as the standard. SEM is indicated by the error bars.

siRNA knock-down data. Although decreases in endogenous *B-FABP* RNA levels were also observed with all combinations of NFI siRNAs tested, fold changes were of considerably lower magnitude than those obtained for endogenous *GFAP*.

Discussion

B-FABP and GFAP are normally found in radial glial cells and astrocytes, respectively, and are co-expressed in malignant glioma tumors and in a subset of malignant glioma cell lines.[20] Previous experiments by us and by others have demonstrated that NFIs are involved in the regulation of the *B-FABP* and *GFAP* genes.[21,22,36,37,46] Tissue-specific expression patterns support a role for NFIs, particularly NFIA, NFIB, and NFIX, in the regulation of genes expressed in glial cells. For example, in postnatal mice, NFIA and NFIB localize primarily to the white matter of the cerebral cortex, suggesting a glial-cell-specific distribution.[28] In humans, NFIA and NFIX are expressed in glial cells where they seem to have greater transactivation capacity than NFIC.[47,48] A role for NFIA and NFIB in glia is supported by the observation that both *Nfia−/−* and *Nfib−/−* mice show losses of midline glial structures, which are accompanied by significant reductions in GFAP levels.[38,41] While brain defects have been reported in *Nfix−/−* mice, there is no indication of glial defects in these mice and *GFAP* RNA levels are not altered.[39]

We show here that all four NFIs are expressed in malignant glioma cell lines, with a trend towards higher levels of *NFIB* RNA in B-FABP/GFAP-positive *versus* B-FABP/GFAP-negative lines. Both ectopic overexpression and RNA interference were

used to investigate the consequence of modulating levels of NFIs on *GFAP*- and *B-FABP*-driven CAT reporter activity. There was general agreement between the two approaches in that NFIA had the strongest positive effect on *GFAP* promoter activity, followed by NFIB and NFIX. The NFI knock-down data further suggested that NFIC plays a negative role in the regulation of *GFAP*. In the case of *B-FABP*, the NFI overexpression and knock-down data both supported a role for NFIC in the down-regulation of *B-FABP* transcription. Knock-down experiments also demonstrated a role for NFIA and NFIB in the up-regulation of *B-FABP* promoter activity, with the most dramatic effect observed when both NFIA and NFIB were targeted by siRNAs. These results suggest that NFIA/NFIB heterodimers may be particularly effective in the activation of *B-FABP* transcription. A summary of the combined data obtained with the NFI knock-down/CAT reporter gene assay is schematically represented in Fig. 12a.

In contrast to ectopic promoter activity, NFI overexpression had no effect on either endogenous GFAP or B-FABP levels, indicating that (i) factors in addition to NFI are required for the expression of these two genes, and (ii) at least some of these factors are in limiting amounts. RNA interference experiments revealed an important role for each NFI in the up-regulation of *GFAP*, with knock-down of each NFI accompanied by dramatic decreases in endogenous *GFAP* RNA (and subsequently protein) levels. These results indicate that although knock-down of one NFI can affect the levels of a different NFI (e.g., up-regulation of NFIA upon NFIB knock-down), members of the NFI family cannot fully compensate for one another in the case of *GFAP*. Thus, all four NFIs, or the ratio of the four NFIs, may play critical roles in *GFAP* regulation.

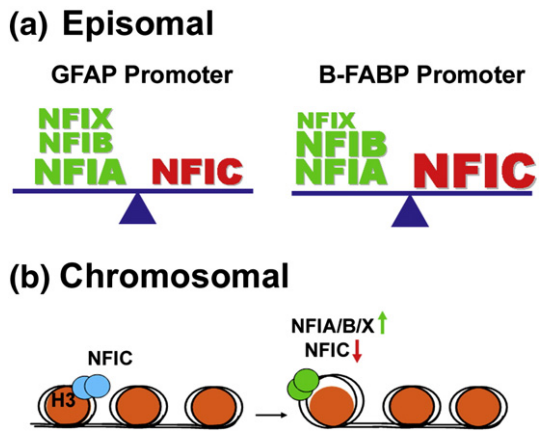

Fig. 12. Model of NFI transcriptional activity. (a) Schematic representation of the relative importance (indicated by font size) of the different NFIs in the up-regulation (green) and down-regulation (red) of *GFAP* and *B-FABP* promoter activity in an episomal context. (b) Roles of NFIs in a chromosomal promoter context using *GFAP* as our model. By binding to histone H3, NFIC (and possibly other NFIs) relaxes the nucleosome structure, thus facilitating binding of NFIs and other transcription factors to *GFAP* upstream sequences.

Although results obtained with the ectopic *versus* endogenous *GFAP* promoter are mostly in agreement, the reduction in endogenous *GFAP* RNA (and protein) levels observed upon NFIC knock-down is inconsistent with the proposed inhibitory role for NFIC in the context of episomal pCAT/GFAP-1708 DNA. Differing results have been reported by others upon comparing promoter activity in an episomal *versus* chromosomal context.[49,50] A likely explanation for this discrepancy is the nucleosomal organization of chromosomal *versus* episomal promoters. While core histones in episomal DNA display similar stoichiometry to that found in chromosomal DNA, episomal templates have fewer H1 linker histones resulting in a lower level of nucleosome assembly (thus facilitating access to transcription factors) compared with chromosomal DNA.[51] In this regard, it is important to note that NFIC has been shown to play a chromatin restructuring role at target promoter sites by specifically binding histone H3 through its proline-rich transcriptional activation domain.[52] A consequence of NFIC knock-down may therefore be reconfiguration of the core nucleosome structure and reduced accessibility of the endogenous *GFAP* promoter to transcription factors (Fig. 12b). We propose that NFIC functions as a transcriptional activator in the context of the endogenous *GFAP* promoter through its chromatin restructuring role and as a transcriptional repressor in the context of the episomal *GFAP* promoter through its classic DNA-binding transcription factor role. In contrast, NFIA, NFIB, and NFIX seem to serve as classic promoter-binding transcriptional activators regardless of *GFAP* promoter context.

Single and combined NFI knock-downs had limited effects on endogenous *B-FABP* RNA levels, with a maximum reduction of ~60% observed in the NFIA/B/C/X quadruple knock-down. The increase in *B-FABP* RNA levels observed upon single NFIB knock-down is likely the consequence of a compensatory increase in NFIA. Furthermore, significant decreases in endogenous B-FABP protein levels were observed only after three rounds of NFI siRNA transfections and may be an indirect consequence of long-term reduction in NFI transcription activity, as NFIs have numerous target genes. The different effects observed at the endogenous *GFAP* and *B-FABP* promoters upon NFI knock-down could be explained by (i) the *B-FABP* transcript being more stable than the *GFAP* transcript, (ii) NFIC not playing a role in chromatin remodeling at the *B-FABP* promoter, and/or (iii) different members of the NFI family being able to compensate for one another at the *B-FABP* but not the *GFAP* promoter.

An important outcome of the NFI knock-down experiments was the discovery that there is cross talk between different members of the NFI family. The consequence of NFIA knock-down was up-regulation of NFIX and *vice versa*, whereas knock-downs of NFIC and NFIB resulted in reduced NFIB and increased NFIA, respectively. These compensatory effects are in keeping with the 2.2-fold increase

in Nfia observed in *Nfib−/−* mice[41] and the 1.3-fold increase in Nfib observed in *Nfia−/−* mice.[53] Thus, the increase in *B-FABP* RNA levels observed in the brains of *Nfia−/−* mice based on microarray analysis[53] may be explained by the compensatory increase in Nfib levels.

ChIP assays have previously demonstrated occupancy of the endogenous *GFAP* promoter by NFIs in primary cortical neuroepithelial cells.[22] Here, we demonstrate that NFIs also occupy the promoter regions of the endogenous *GFAP* and *B-FABP* genes in U251 malignant glioma cells. *In vitro* gel-shift experiments using nuclear extracts from B-FABP/GFAP-negative T98 and B-FABP/GFAP-positive U251 cell lines revealed binding of NFIs to NFI recognition sites in the *GFAP* and *B-FABP* promoters. Retarded bands of similar intensities were observed with both extracts, in spite of the fact that T98 has lower levels of *NFI* RNA compared with U251. Possible explanations for this apparent discrepancy are that (i) *NFI* RNA levels may not reflect NFI protein levels in T98 and U251 cells, (ii) hyperphosphorylation of NFIs in T98 may stabilize the protein, or (iii) hyperphosphorylated NFIs may bind more tightly to NFI recognition sites *in vitro* (although the literature would suggest otherwise).[35]

To investigate whether different members of the NFI family can preferentially bind to the NFI recognition sites found upstream of the *GFAP* and *B-FABP* promoters, we carried out gel shifts with nuclear extracts prepared from T98 cells overexpressing individual NFIs. NFIX showed the least discrimination for NFI recognition sites, effectively binding to the three G-br binding sites in the *GFAP* promoter and the three B-br binding sites in the *B-FABP* promoter *in vitro*. NFIA could also bind to all six NFI recognition sites, although only weakly to B-br3. NFIC seemed to recognize B-br binding sites much more efficiently than G-br sites, with strong binding to all three B-br sites. NFIB showed the highest degree of discrimination, binding to G-br2, B-br1, B-br2, and, to a lesser extent, G-br1.

We examined the sequences of the *B-FABP* and *GFAP* NFI binding sites in an attempt to link DNA binding by the more discriminatory NFIs to one or more specific target sequences. We found that none of the six NFI binding sites (B-br1, B-br2, B-br3, G-br1, G-br2, and G-br3) were identical with one another and none were identical with the 15-bp NFI consensus binding site $TTGGCN_5GCCAA$. The six NFI binding sites each had 1- to 3-bp deviations from the consensus sequence. With the exception of B-br2 (4-bp internal spacer), all had a 5-bp internal spacer. Interestingly, NFI binding sites most closely resembling the consensus sequence (e.g., B-br2, with a single base-pair substitution at position 1; G-br2, with 2-ase-pairbp substitutions at positions 11 and 12) were bound equally well by all four NFIs. With the exception of B-br1, NFI binding sites with 3-bp substitutions (e.g., G-br3 and B-br3) demonstrated the highest degree of differential binding.

There was little correlation between the ability of NFIs to bind to G-br and B-br sites and NFI transcription activity. For example, even though NFIX and NFIA both formed complexes with all six G-br/B-br oligonucleotides, NFIX knock-down had little effect on *B-FABP*-driven CAT activity whereas NFIA knock-down decreased the activity of both the *GFAP* and the *B-FABP* promoters. These results are in agreement with other reports indicating that transcription factor binding affinity is a poor predictor of transcription activity.[54,55] Furthermore, mutation of individual or combined G-br recognition sites suggests context-dependent binding by NFIs, with NFIB knock-down having the strongest effect on G-br1 in the context of the −168-bp upstream region and NFIA knock-down resulting in a significant decrease in CAT activity in the context of the −1708-bp upstream region mutated at G-br2* and G-br3* (leaving only the G-br1 intact). It is clear that factors other than the ability to bind NFI consensus sites *in vitro* are important for NFI transactivation, including recruitment of transcriptional cofactors and/or cooperative interactions with different members of the NFI family or factors that bind to neighboring elements.

A number of transcription factors and pathways have been implicated in *B-FABP* and *GFAP* regulation. For example, *B-FABP* has recently been shown to be a downstream target of the Notch effector CBF1 in radial glial cells and of Pax6 in the neuroepithelial cells of the developing rat cortex.[56,57] Previous work has identified a radial glial element located within 800 bp of the *B-FABP* transcription start site[58] and a hybrid Pbx/POU binding site at −370 bp.[59] Similarly, activator protein-1[46] and the transforming growth factor-β, mitogen-activated protein kinase, phosphatidylinositol 3-kinase, and Smad pathways[60] are believed to be involved in the regulation of *GFAP* in astrocytes. Our data indicate that NFIs, in conjunction with other transcription factors, should be added to the list of important transcription factors involved in the control of *B-FABP* and *GFAP* expression.

In conclusion, our data demonstrate the importance of all four NFIs, in conjunction with NFI phosphorylation, in the regulation of *GFAP* and *B-FABP* promoter activity in malignant glioma cells. We show that there is cross talk between the different members of the NFI family and that particular NFIs or combinations of NFIs (either in the form of homodimers or in the form of heterodimers) are more effective at up-regulating or down-regulating *GFAP* and *B-FABP* promoter activity. Of note, significant differences in NFI transcriptional activity were observed depending on whether the promoter was in a chromosomal or episomal configuration, likely reflecting a dual role for NFIs in chromatin remodeling and as classic transcription factors. Future work will involve ChIP to study the *in vivo* occupancy of individual NFIs at the endogenous *GFAP* and *B-FABP* promoters and to identify additional NFI target genes in malignant glioma.

Materials and Methods

Cell lines, constructs, and transfections

The sources of the human malignant glioma cell lines included in this analysis have been previously described,[20] with the exception of M103, which was established by Dr. Rufus Day (Department of Oncology, University of Alberta) from a malignant glioma biopsy. Cells were cultured in Dulbecco's modification of Eagle's minimum essential medium supplemented with 10% fetal calf serum, penicillin (100 U/ml), and streptomycin (100 μg/ml).

The pCHNFI expression vectors (pCH, pCHNFIA, pCHNFIB, pCHNFIC, and pCHNFIX) were obtained from Dr. R. Gronostajski (Case Western Reserve University). The following CAT reporter gene constructs were used for the *B-FABP* and *GFAP* promoter assays: (i) pCAT/B-FABP-1785 containing 5′ *B-FABP* flanking DNA from −1785 to +20 bp, (ii) pCAT/GFAP-168 with 5′ *GFAP* flanking DNA from −168 to +8 bp, and (iii) pCAT/GFAP-1708 with 5′ *GFAP* flanking DNA from −1708 to +8 bp. Plasmids were introduced into the U251 malignant glioma cell line by polyethylenimine (Polysciences, Inc.)-mediated DNA transfection. Cells were harvested 60 h after transfection, and a fixed portion (75% or 80% depending on the experiment) was used to prepare lysates for CAT activity. CAT activity was measured using 1/10 of the lysates following the protocol supplied by Promega. Acetylated [^{14}C]chloramphenicol was measured (in cpm) using a scintillation counter. To control for plate-to-plate variation in amount of transfected DNA, a fixed portion of the cells (20% or 25% depending on the experiment) was used to isolate nonintegrated DNA.[45] The DNA was restriction enzyme digested, electrophoresed on a 1% agarose gel, transferred onto nitrocellulose, and probed with radioactively labeled pCAT basic DNA.

Single, double, and triple mutations of the three NFI binding sites (G-br1, G-br2, and G-br3) located upstream of the *GFAP* transcription start site were generated by sequential PCR.[61] For single mutations, complementary oligonucleotides carrying 2-bp substitutions (GG→AA) for each of G-br1, G-br2, and G-br3 were used in conjunction with upstream and downstream pCAT-1708 primers to generate fragments corresponding to the 1708-bp *GFAP* promoter region. *GFAP* promoter fragments mutated at G-br1 (G-br1*), G-br2 (G-br2*), or G-br3 (G-br3*) (Fig. 2c) were inserted in the pCAT basic vector. The double mutant (G-br2*/G-br3*) was generated from the G-br2* mutant, whereas the triple mutant (G-br1*/G-br2*/G-br3*) was generated from the G-br2*/G-br3* double mutant. Sequence analysis revealed that all mutated sites were as expected, except for the G-br2 site in the triple mutant, where GG was converted to AG instead of AA.

Northern blot analysis

Conditions for poly(A)$^+$ RNA isolation, probe hybridization, washing filters, and stripping filters have been described.[20] The following probes were used for hybridization: 1.8-kb EcoRI/NcoI cDNA insert from human *NFIA* EST clone #45182 (Genome Systems, Inc.); 600-bp human *NFIB* cDNA corresponding to sequences 934 to 1521 of U85193 (GenBank accession number) generated by PCR amplification; 800-bp EcoRI/HindIII cDNA insert from human *NFIC* EST clone #129328; 700-bp PstI/XhoI cDNA insert from human *NFIX* EST clone #154038; 500-bp EcoRI/EcoRV *GFAP* cDNA insert (GenBank M78090) (American Type Culture Collection, Rockville, MD); 700-bp *B-FABP* cDNA insert[20]; and 500-bp mouse actin cDNA.[62]

Quantitative RT-PCR analysis

Total RNA was isolated using the RNeasy Plus Kit (Qiagen) and first-strand cDNA synthesized from 3.5 μg of RNA using Superscript reverse transcriptase (Invitrogen). The cDNA was amplified using TaqMan Universal PCR Master Mix and gene-specific oligonucleotides (NFIA, Hs00325656_m1; NFIB, Hs00232149_m1; NFIC, Hs00907819_m1; NFIX, Hs00958849_m1; GFAP, Hs00157674_m1; B-FABP, Hs00361426_m1; GAPDH, Hs99999905_m1) labeled at the 5′ end with the fluorescent reporter dye FAM (Applied Biosystems) (ABI 7900HT Fast Real-Time PCR System). All cDNAs were run in triplicate, and the data were normalized using *GAPDH*.

Western blot analysis

Nuclear extracts were prepared as described.[63] Whole-cell extracts were prepared by resuspending the cells in 50 mM Tris–HCl (pH 7.5), 150 mM NaCl, 0.5% sodium deoxycholate, 1% Nonidet P-40, 25 mM sodium pyrophosphate, 50 mM sodium fluoride, 1× Complete protease inhibitor (Roche), 1 mM PMSF, and lysing cells on ice for 20 min. Protein extracts were electrophoresed in polyacrylamide–SDS gels followed by electroblotting onto polyvinylidene fluoride (PVDF) or nitrocellulose membranes. Blots were immunostained with mouse anti-HA antibody (Sigma) (1:10,000), mouse anti-proliferating cell nuclear antigen antibody (BD Biosciences) (1:1000), rabbit anti-B-FABP[20] (1:2000), mouse anti-GFAP antibody (BD Biosciences) (1:10,000), and mouse anti-actin antibody (Sigma) (1:50,000). Primary antibodies were detected with horseradish-peroxidase-conjugated secondary antibodies (Jackson ImmunoResearch Biotech) using the ECL detection system (Amersham Biosciences).

Gel-shift assay

The gel-shift assay was carried out as described.[64] The sequences of the *B-FABP* (B-br1, B-br2, and B-br3) and *GFAP* (G-br1, G-br2, and G-br3) NFI binding regions are listed in Fig. 2. Complementary oligonucleotides were annealed and radiolabeled by filling in with Klenow polymerase in the presence of [α-^{32}P]deoxycytidine triphosphate. Site-directed mutagenesis of G-br1, G-br2, and G-br3 was carried out by substituting the conserved GG residues at positions 3 and 4 of the NFI consensus binding site with AA (Fig. 2). NFI, Sp1, and AP-2 double-stranded oligonucleotides were generated by annealing 5′-ATTTTGGCTTGAAGCCAATATG-3′ and 5′-CATATTGGCTTCAAGCCAAAAT-3′ (NFI consensus binding site is underlined), 5′-GATCGATCGGGGCGGGGCGATC-3′ and 5′-GATCGCCCCGCCCCGATCGATC-3′ (Sp1), and 5′-GATCGAACTGACCGCCCGCGGCCCGT-3′ and 3′-ACGGGCCGCGGGCGGTCAGTTCGATC-3′ (AP-2).

Nuclear extracts from T98, U251, as well as T98 cells transiently transfected with 10 μg of pCH control vector or pCH HA-tagged NFIA, NFIB, NFIC, and NFIX expression constructs were prepared as described earlier. Nuclear extracts (4 μg for T98 and U251 and 1 μg for transfected cells) were preincubated in the presence of 1.25 μg of poly (dI–dC) in binding buffer [20 mM Hepes (pH 7.9), 20 mM KCl, 1 mM spermidine, 10 mM dithiothreitol, 10%

Table 1. Sequences of primers used for ChIP analysis

Fragment	Forward sequence (5′–3′)	Reverse sequence (5′–3′)
G-br1	GTCCTCTTGCTTCAGCGG	TGGGCTAGACTGGCGATG
G-br2	CAGGGCCTCCTCTTCATG	TAGAGCCTTGTTCTCCACC
G-br3	GGACGCTGCTCTGACAGA	CACTGGGCATGAAGAGGAG
G-br2/3	CAGACCTGGCAGCATTGG	CTGCTCAATGGGCTTCTCG
B-br1	GATTGGAGCCTCACTCGAG	CTGCAGCTCAGAAGACCC
B-br2	GCATAAGGGCTGTAGTGTG	CAGTGTCCCTCTTTCCAAG
B-br3	GTCTGAGATTGCCTTTGCC	GTTAGCGGAGTAGGTCGAG
B-br1/2/3	CGAACCTGAAAGCCCTTCT	GCTCCTGCCTTCTTATTTGG
GAPDH	GAACCAGCACCGATCACC	CCAGCCCAAGGTCTTGAG

glycerol, 0.1% Nonidet P-40] for 10 min at room temperature. When included, a 100× molar excess of unlabeled competitor oligonucleotide was added during the preincubation stage. For supershift experiments, 1 μl anti-HA antibody (clone H7, Sigma), 1 μl anti-NFI antibody (obtained from Dr. Naoko Tanese, NYU Medical Center, New York, NY), 1 μl anti-AP-2 antibody (negative control) (Santa Cruz Biotechnology, Inc.), or 1 μl anti-Pax6 antibody (negative control) (Developmental Studies Hybridoma Bank maintained by the University of Iowa under contract NO1-HD-7-3263 from the National Institute of Child Health and Human Development) was included in the preincubation reaction. Labeled DNA was added and incubated for 20 min at room temperature. DNA–protein complexes were resolved on a 6% polyacrylamide gel in 0.5× TBE (Tris–borate–EDTA).

Knock-down of endogenous NFIs

The following Stealth siRNAs were used to transfect U251 cells: NM_005595_stealth_919 targeting 5′-GAAAGUUCUUCAUACUACAGCAUGA-3′ of NFIA, NM_005596_stealth_1020 targeting 5′-AAGCCACAAUGAUCCUGCCAAGAAU-3′ of NFIB, NM_005597_stealth_1045 targeting 5′-CAGAGAUGGACAAGUCACCAUUCAA-3′ of NFIC, NM_002501_stealth_752 targeting 5′-GAGAGUAUCACAGACUCCUGUUGCA-3′ of NFIX, and control siRNA (cat. nos. 12935-200 and 12935-300) (Invitrogen). Cells were transfected with 10 nM Stealth siRNAs targeting individual *NFI* genes using the RNAi-MAX Lipofectamine reagent (Invitrogen). Where appropriate, cells were transfected the following day with either GFAP- or B-FABP-CAT constructs using the polyethylenimine reagent. Cells were harvested 60 h after the last transfection. When multiple rounds of siRNA transfections were carried out, 9/10 of cells were harvested at confluency and 1/10 of the cells were replated and retransfected.

Chromatin immunoprecipitation

ChIP was carried out according to Pillai *et al.*[65] U251 cells were cross-linked with 1% formaldehyde for 20 min at room temperature. The cross-linking reaction was terminated with the addition of glycine to a final concentration of 0.125 M. Cells were harvested by cell scraping in 1× phosphate-buffered saline, washed, and resuspended in lysis buffer [44 mM Tris–HCl (pH 8.0), 1% SDS, 10 mM EDTA (ethylenediaminetetraacetic acid), 1 mM PMSF, and 1× Complete protease inhibitor cocktail]. Cells were sonicated for 3×30 s at 30% output (model 300VT, Ultrasonic Homogenizer, BioLogics, Inc.). After sonication, ChIP lysate was precleared by incubation with protein A–Sepharose beads (GE Healthcare). The precleared ChIP lysate was incubated with either 3 μg of rabbit anti-NFI antibody (N-20; Santa Cruz Biotechnology) or 3 μg of rabbit IgG (negative control) at 4 °C overnight. Protein A–Sepharose beads were added to the ChIP lysate–antibody mixture and incubated for an additional 2 h at 4 °C. Beads were washed and protein–DNA complexes were eluted in 0.1 M $NaHCO_3$, 1% SDS, 5 mM NaCl. Cross-links were reversed by incubation at 65 °C for 5 h. Proteins were digested with proteinase K and the DNA was purified using a DNA purification kit (Marligen Rapid PCR purification system). Primers used to amplify specific regions of the *GFAP, B-FABP,* and *GAPDH* (glyceraldehyde-3-phosphate dehydrogenase; negative control) promoters are listed in Table 1. PCR conditions were 95 °C for 2 min, followed by 30 cycles at 95 °C for 30 s, 55 °C for 30 s, and 72 °C for 30 s, followed by an additional 7-min incubation at 72 °C. PCR products were resolved on a 1% agarose gel and detected using ethidium bromide.

Acknowledgements

We thank Mary Packer for expert technical assistance. We are grateful to Dr. Richard Gronostajski for his gift of the pCHNFI expression constructs and to Dr. Naoko Tanese for the anti-NFI antibody used in the supershift experiments. This work was supported by the National Cancer Institute of Canada with funds from the Cancer Research Society and by the Alberta Cancer Research Institute. M.B. is funded by an Alberta Cancer Research Institute Cyril Kay Graduate Studentship.

Supplementary Data

Supplementary data associated with this article can be found, in the online version, at doi:10.1016/j.jmb.2009.06.041

References

1. Bohnen, N. I. & Radhakrishnan, K. (1997). *Cancer of the Nervous System.* Blackwell Science, Cambridge, MA.
2. Eng, L. F. & Rubinstein, L. J. (1978). Contribution of immunohistochemistry to diagnostic problems of human cerebral tumors. *J. Histochem. Cytochem.* **26**, 513–522.

3. van der Meulen, J. D., Houthoff, H. J. & Ebels, E. J. (1978). Glial fibrillary acidic protein in human gliomas. *Neuropathol. Appl. Neurobiol.* **4**, 177–190.
4. Chen, W. J. & Liem, R. K. (1994). Reexpression of glial fibrillary acidic protein rescues the ability of astrocytoma cells to form processes in response to neurons. *J. Cell Biol.* **127**, 813–823.
5. Engelhard, H. H., Duncan, H. A. & Dal Canto, M. (1997). Molecular characterization of glioblastoma cell differentiation. *Neurosurgery*, **41**, 886–896; discussion 896–897.
6. Langlois, A., Lee, S., Kim, D. S., Dirks, P. B. & Rutka, J. T. (2002). p16(ink4a) and retinoic acid modulate rhoA and GFAP expression during induction of a stellate phenotype in U343 MG-A astrocytoma cells. *Glia*, **40**, 85–94.
7. Murphy, K. G., Hatton, J. D. & U, H. S. (1998). Role of glial fibrillary acidic protein expression in the biology of human glioblastoma U-373MG cells. *J. Neurosurg.* **89**, 997–1006.
8. Rutka, J. T., Hubbard, S. L., Fukuyama, K., Matsuzawa, K., Dirks, P. B. & Becker, L. E. (1994). Effects of antisense glial fibrillary acidic protein complementary DNA on the growth, invasion, and adhesion of human astrocytoma cells. *Cancer Res.* **54**, 3267–3272.
9. Rutka, J. T. & Smith, S. L. (1993). Transfection of human astrocytoma cells with glial fibrillary acidic protein complementary DNA: analysis of expression, proliferation, and tumorigenicity. *Cancer Res.* **53**, 3624–3631.
10. Feng, L., Hatten, M. E. & Heintz, N. (1994). Brain lipid-binding protein (BLBP): a novel signaling system in the developing mammalian CNS. *Neuron*, **12**, 895–908.
11. Kurtz, A., Zimmer, A., Schnutgen, F., Bruning, G., Spener, F. & Muller, T. (1994). The expression pattern of a novel gene encoding brain-fatty acid binding protein correlates with neuronal and glial cell development. *Development*, **120**, 2637–2649.
12. Culican, S. M., Baumrind, N. L., Yamamoto, M. & Pearlman, A. L. (1990). Cortical radial glia: identification in tissue culture and evidence for their transformation to astrocytes. *J. Neurosci.* **10**, 684–692.
13. Schmechel, D. E. & Rakic, P. (1979). A Golgi study of radial glial cells in developing monkey telencephalon: morphogenesis and transformation into astrocytes. *Anat. Embryol.* **156**, *115–152.*
14. Anthony, T. E., Klein, C., Fishell, G. & Heintz, N. (2004). Radial glia serve as neuronal progenitors in all regions of the central nervous system. *Neuron*, **41**, 881–890.
15. Malatesta, P., Hack, M. A., Hartfuss, E., Kettenmann, H., Klinkert, W., Kirchhoff, F. & Gotz, M. (2003). Neuronal or glial progeny: regional differences in radial glia fate. *Neuron*, **37**, 751–764.
16. Noctor, S. C., Flint, A. C., Weissman, T. A., Wong, W. S., Clinton, B. K. & Kriegstein, A. R. (2002). Dividing precursor cells of the embryonic cortical ventricular zone have morphological and molecular characteristics of radial glia. *J. Neurosci.* **22**, 3161–3173.
17. Kaloshi, G., Mokhtari, K., Carpentier, C., Taillibert, S., Lejeune, J., Marie, Y. *et al.* (2007). FABP7 expression in glioblastomas: relation to prognosis, invasion and EGFR status. *J. Neuro-Oncol.* **84**, 245–248.
18. Liang, Y., Diehn, M., Watson, N., Bollen, A. W., Aldape, K. D., Nicholas, M. K. *et al.* (2005). Gene expression profiling reveals molecularly and clinically distinct subtypes of glioblastoma multiforme. *Proc. Natl Acad. Sci. USA*, **102**, 5814–5819.
19. Mita, R., Coles, J. E., Glubrecht, D. D., Sung, R., Sun, X. & Godbout, R. (2007). B-FABP-expressing radial glial cells: the malignant glioma cell of origin? *Neoplasia*, **9**, 734–744.
20. Godbout, R., Bisgrove, D. A., Shkolny, D. & Day, R. S. (1998). Correlation of B-FABP and GFAP expression in malignant glioma. *Oncogene*, **16**, 1955–1962.
21. Bisgrove, D. A., Monckton, E. A., Packer, M. & Godbout, R. (2000). Regulation of brain fatty acid-binding protein expression by differential phosphorylation of nuclear factor I in malignant glioma cell lines. *J. Biol. Chem.* **275**, 30668–30676.
22. Cebolla, B. & Vallejo, M. (2006). Nuclear factor-I regulates glial fibrillary acidic protein gene expression in astrocytes differentiated from cortical precursor cells. *J. Neurochem.* **97**, 1057–1070.
23. Gopalan, S. M., Wilczynska, K. M., Konik, B. S., Bryan, L. & Kordula, T. (2006). Nuclear factor-1-X regulates astrocyte-specific expression of the α1-antichymotrypsin and glial fibrillary acidic protein genes. *J. Biol. Chem.* **281**, 13126–13133.
24. Qian, F., Kruse, U., Lichter, P. & Sippel, A. E. (1995). Chromosomal localization of the four genes (NFIA, B, C, and X) for the human transcription factor nuclear factor I by FISH. *Genomics*, **28**, 66–73.
25. Gronostajski, R. M. (2000). Roles of the NFI/CTF gene family in transcription and development. *Gene*, **249**, 31–45.
26. Kruse, U. & Sippel, A. E. (1994). Transcription factor nuclear factor I proteins form stable homo- and heterodimers. *FEBS Lett.* **348**, 46–50.
27. Roulet, E., Bucher, P., Schneider, R., Wingender, E., Dusserre, Y., Werner, T. & Mermod, N. (2000). Experimental analysis and computer prediction of CTF/NFI transcription factor DNA binding sites. *J. Mol. Biol.* **297**, 833–848.
28. Chaudhry, A. Z., Lyons, G. E. & Gronostajski, R. M. (1997). Expression patterns of the four nuclear factor I genes during mouse embryogenesis indicate a potential role in development. *Dev. Dyn.* **208**, 313–325.
29. Amemiya, K., Traub, R., Durham, L. & Major, E. O. (1992). Adjacent nuclear factor-1 and activator protein binding sites in the enhancer of the neurotropic JC virus. A common characteristic of many brain-specific genes. *J. Biol. Chem.* **267**, 14204–14211.
30. Deneen, B., Ho, R., Lukaszewicz, A., Hochstim, C. J., Gronostajski, R. M. & Anderson, D. J. (2006). The transcription factor NFIA controls the onset of gliogenesis in the developing spinal cord. *Neuron*, **52**, 953–968.
31. Inoue, T., Tamura, T., Furuichi, T. & Mikoshiba, K. (1990). Isolation of complementary DNAs encoding a cerebellum-enriched nuclear factor I family that activates transcription from the mouse myelin basic protein promoter. *J. Biol. Chem.* **265**, 19065–19070.
32. Kumar, K. U., Pater, A. & Pater, M. M. (1993). Human JC virus perfect palindromic nuclear factor 1-binding sequences important for glial cell-specific expression in differentiating embryonal carcinoma cells. *J. Virol.* **67**, 572–576.
33. Major, E. O., Amemiya, K., Elder, G. & Houff, S. A. (1990). Glial cells of the human developing brain and B cells of the immune system share a common DNA binding factor for recognition of the regulatory sequences of the human polyomavirus, JCV. *J. Neurosci. Res.* **27**, 461–471.
34. Shu, T., Butz, K. G., Plachez, C., Gronostajski, R. M. & Richards, L. J. (2003). Abnormal development of forebrain midline glia and commissural projections in Nfia knock-out mice. *J. Neurosci.* **23**, 203–212.

35. Yang, B. S., Gilbert, J. D. & Freytag, S. O. (1993). Overexpression of Myc suppresses CCAAT transcription factor/nuclear factor 1-dependent promoters *in vivo*. *Mol. Cell. Biol.* **13**, 3093–3102.
36. Besnard, F., Brenner, M., Nakatani, Y., Chao, R., Purohit, H. J. & Freese, E. (1991). Multiple interacting sites regulate astrocyte-specific transcription of the human gene for glial fibrillary acidic protein. *J. Biol. Chem.* **266**, 18877–18883.
37. Masood, K., Besnard, F., Su, Y. & Brenner, M. (1993). Analysis of a segment of the human glial fibrillary acidic protein gene that directs astrocyte-specific transcription. *J. Neurochem.* **61**, 160–166.
38. das Neves, L., Duchala, C. S., Tolentino-Silva, F., Haxhiu, M. A., Colmenares, C., Macklin, W. B. *et al.* (1999). Disruption of the murine nuclear factor I-A gene (Nfia) results in perinatal lethality, hydrocephalus, and agenesis of the corpus callosum. *Proc. Natl Acad. Sci. USA*, **96**, 11946–11951.
39. Driller, K., Pagenstecher, A., Uhl, M., Omran, H., Berlis, A., Grunder, A. & Sippel, A. E. (2007). Nuclear factor I X deficiency causes brain malformation and severe skeletal defects. *Mol. Cell. Biol.* **27**, 3855–3867.
40. Steele-Perkins, G., Butz, K. G., Lyons, G. E., Zeichner-David, M., Kim, H. J., Cho, M. I. & Gronostajski, R. M. (2003). Essential role for NFI-C/CTF transcription-replication factor in tooth root development. *Mol. Cell. Biol.* **23**, 1075–1084.
41. Steele-Perkins, G., Plachez, C., Butz, K. G., Yang, G., Bachurski, C. J., Kinsman, S. L. *et al.* (2005). The transcription factor gene Nfib is essential for both lung maturation and brain development. *Mol. Cell. Biol.* **25**, 685–698.
42. Campbell, C. E., Piper, M., Plachez, C., Yeh, Y. T., Baizer, J. S., Osinski, J. M. *et al.* (2008). The transcription factor Nfix is essential for normal brain development. *BMC Dev. Biol.* **8**, 52.
43. Namihira, M., Kohyama, J., Semi, K., Sanosaka, T., Deneen, B., Taga, T. & Nakashima, K. (2009). Committed neuronal precursors confer astrocytic potential on residual neural precursor cells. *Dev. Cell*, **16**, 245–255.
44. Gronostajski, R. M. (1987). Site-specific DNA binding of nuclear factor I: effect of the spacer region. *Nucleic Acids Res.* **15**, 5545–5559.
45. Hirt, B. (1967). Selective extraction of polyoma DNA from infected mouse cell cultures. *J. Mol. Biol.* **26**, 365–369.
46. Gopalan, S. M., Wilczynska, K. M., Konik, B. S., Bryan, L. & Kordula, T. (2006). Astrocyte-specific expression of the α1-antichymotrypsin and glial fibrillary acidic protein genes requires activator protein-1. *J. Biol. Chem.* **281**, 1956–1963.
47. Krebs, C. J., Dey, B. & Kumar, G. (1996). The cerebellum-enriched form of nuclear factor I is functionally different from ubiquitous nuclear factor I in glial-specific promoter regulation. *J. Neurochem.* **66**, 1354–1361.
48. Sumner, C., Shinohara, T., Durham, L., Traub, R., Major, E. O. & Amemiya, K. (1996). Expression of multiple classes of the nuclear factor-1 family in the developing human brain: differential expression of two classes of NF-1 genes. *J. NeuroVirol.* **2**, 87–100.
49. Archer, T. K., Lefebvre, P., Wolford, R. G. & Hager, G. L. (1992). Transcription factor loading on the MMTV promoter: a bimodal mechanism for promoter activation. *Science*, **255**, 1573–1576.
50. Gerber, A. N., Klesert, T. R., Bergstrom, D. A. & Tapscott, S. J. (1997). Two domains of MyoD mediate transcriptional activation of genes in repressive chromatin: a mechanism for lineage determination in myogenesis. *Genes Dev.* **11**, 436–450.
51. Hebbar, P. B. & Archer, T. K. (2008). Altered histone H1 stoichiometry and an absence of nucleosome positioning on transfected DNA. *J. Biol. Chem.* **283**, 4595–4601.
52. Alevizopoulos, A., Dusserre, Y., Tsai-Pflugfelder, M., von der Weid, T., Wahli, W. & Mermod, N. (1995). A proline-rich TGF-β-responsive transcriptional activator interacts with histone H3. *Genes Dev.* **9**, 3051–3066.
53. Wong, Y. W., Schulze, C., Streichert, T., Gronostajski, R. M., Schachner, M. & Tilling, T. (2007). Gene expression analysis of nuclear factor I-A deficient mice indicates delayed brain maturation. *Genome Biol.* **8**, R72.
54. Bachurski, C. J., Yang, G. H., Currier, T. A., Gronostajski, R. M. & Hong, D. (2003). Nuclear factor I/thyroid transcription factor 1 interactions modulate surfactant protein C transcription. *Mol. Cell. Biol.* **23**, 9014–9024.
55. Osada, S., Matsubara, T., Daimon, S., Terazu, Y., Xu, M., Nishihara, T. & Imagawa, M. (1999). Expression, DNA-binding specificity and transcriptional regulation of nuclear factor 1 family proteins from rat. *Biochem. J.* **342**(Pt. 1), 189–198.
56. Anthony, T. E., Mason, H. A., Gridley, T., Fishell, G. & Heintz, N. (2005). Brain lipid-binding protein is a direct target of Notch signaling in radial glial cells. *Genes Dev.* **19**, 1028–1033.
57. Arai, Y., Funatsu, N., Numayama-Tsuruta, K., Nomura, T., Nakamura, S. & Osumi, N. (2005). Role of Fabp7, a downstream gene of Pax6, in the maintenance of neuroepithelial cells during early embryonic development of the rat cortex. *J. Neurosci.* **25**, 9752–9761.
58. Feng, L. & Heintz, N. (1995). Differentiating neurons activate transcription of the brain lipid-binding protein gene in radial glia through a novel regulatory element. *Development (Cambridge, U.K.)*, **121**, 1719–1730.
59. Josephson, R., Muller, T., Pickel, J., Okabe, S., Reynolds, K., Turner, P. A. *et al.* (1998). POU transcription factors control expression of CNS stem cell-specific genes. *Development (Cambridge, U.K.)*, **125**, 3087–3100.
60. Romao, L. F., Sousa Vde, O., Neto, V. M. & Gomes, F. C. (2008). Glutamate activates GFAP gene promoter from cultured astrocytes through TGF-β1 pathways. *J. Neurochem.* **106**, 746–756.
61. Cormack, B. & Castano, I. (2002). Introduction of point mutations into cloned genes. *Methods Enzymol.* **350**, 199–218.
62. Minty, A. J., Caravatti, M., Robert, B., Cohen, A., Daubas, P., Weydert, A. *et al.* (1981). Mouse actin messenger RNAs. Construction and characterization of a recombinant plasmid molecule containing a complementary DNA transcript of mouse α-actin mRNA. *J. Biol. Chem.* **256**, 1008–1014.
63. Dignam, J. D., Lebovitz, R. M. & Roeder, R. G. (1983). Accurate transcription initiation by RNA polymerase II in a soluble extract from isolated mammalian nuclei. *Nucleic Acids Res.* **11**, 1475–1489.
64. O'Brien, R. M., Noisin, E. L., Suwanichkul, A., Yamasaki, T., Lucas, P. C., Wang, J. C. *et al.* (1995). Hepatic nuclear factor 3- and hormone-regulated expression of the phosphoenolpyruvate carboxykinase and insulin-like growth factor-binding protein 1 genes. *Mol. Cell. Biol.* **15**, 1747–1758.
65. Pillai, S., Dasgupta, P. & Chellappan, S. P. (2009). Chromatin immunoprecipitation assays: analyzing transcription factor binding and histone modifications *in vivo*. *Methods Mol. Biol.* **523**, 323–339.